Gene Regulatory Mechanisms of *Drosophila* Embryonic Motor Neuron Development

by

Katherine Helena Fisher

A dissertation accepted and approved in partial fulfillment of the

requirements for the degree of

Doctor of Philosophy

in Biology

Dissertation Committee:

Dr. Karen Guillemin, Chair

Dr. Chris Doe, Advisor

Dr. Judith Eisen, Core Member

Dr. Tory Herman, Core Member

Dr. Matt Smear, Institutional Representative

University of Oregon

Summer 2025

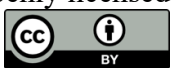

DISSERTATION ABSTRACT

Katherine Helena Fisher

Doctor of Philosophy in Biology

Title: Gene Regulatory Mechanisms of *Drosophila* embryonic motor neuron development

Abstract

Neural progenitors give rise to distinct populations of neurons throughout development. *Drosophila* larval neural progenitors, neuroblasts (NBs), express temporal gradients of transcription factors and RNA-binding proteins to establish neuronal diversity. The function of temporal transcription factors (TTFs) is well-studied in larval neural development. Several factors are expressed early in larval development, including Imp and Chinmo, while other factors are expressed later, including Syp, Mamo, and Broad, and an additional TF, Sequoia, is expressed throughout larval development. While the gene regulatory network of these factors has been thoroughly characterized in larvae, little is known about their expression or function in embryonic CNS development. Here we characterize the expression of early and late temporal factors in embryonic development. We find that Imp and Sequoia are expressed in neuroblasts, with a gradient of low-to-high expression in aging neuroblasts, which is maintained in post-mitotic neurons. Interestingly, the embryonic Imp gradient is opposite the larval Imp gradient. The embryonic Sequoia gradient also contrasts larval expression where no gradient is detected. Another larval early factor, Chinmo, is expressed in all post-mitotic neurons, but not in a gradient. The late factors Mamo, EcR, Syp, and Broad are not expressed in embryos, with the exception of sparse Broad expression. Loss-of-function experiments showed that Imp is required for Chinmo expression. Intriguingly, loss of Chinmo -- but not Imp -- derepresses Syp. Finally, we tested whether Imp and Chinmo are required for motor neuron identity or morphology. We found that Imp, Chinmo, and Sequoia do not have a role in specifying motor neuron identity, but Imp and Chinmo have a later function in promoting motor axon targeting to the correct body wall muscle, and Chinmo is also required to prevent ectopic motor neuron dendrite projections. Together, these results show that the temporal factors are regulated differently in embryos and larvae, and that Imp and Chinmo are required for proper motor neuron axon or dendrite projections.

This dissertation includes previously published and co-authored materials.

CURRICULUM VITAE

NAME OF AUTHOR: Katherine Helena Fisher

GRADUATE AND UNDERGRADUATE SCHOOLS ATTENDED:

University of Oregon, Eugene
Indiana University Bloomington

DEGREES AWARDED:

Doctor of Philosophy, Biology, 2025, University of Oregon
Bachelor's of Science, Biology, 2019, Indiana University Bloomington

AREAS OF SPECIAL INTEREST:

Developmental Neurobiology
Embryo Patterning

PROFESSIONAL EXPERIENCE:

Graduate Researcher, University of Oregon, 2023-2025
Laboratory of Dr. Chris Q. Doe

Graduate Researcher, University of Oregon, 2019-2023
Laboratory of Dr. Daniel Grimes

Graduate Teaching Assistant, University of Oregon, 2019-2020

Undergraduate Researcher, Indiana University Bloomington, 2015-2019
Laboratory of Dr. W. Daniel Tracey

Summer Undergraduate Research Scholar, HHMI Janelia Research Campus, 2018
Laboratory of Dr. Tzumin Lee

NSF Summer Undergraduate Research Fellow, Marine Biological Laboratory, 2017
Laboratory of Dr. Marko Horb

Undergraduate Teaching Assistant, Indiana University Bloomington, 2017-2019

GRANTS, AWARDS, AND HONORS:

National Institutes of Health National Research Service Award F31, Genetic Dissection of fluid flow signaling in Left-Right patterning of zebrafish (1F31HD108945), University of Oregon, 2022-2025

American Heart Association Predoctoral Fellowship, Genetic Dissection of fluid flow signaling in Left-Right patterning of zebrafish (#909113, declined), 2022-2024, University of Oregon

National Science Foundation Graduate Research Fellowship, Understanding differentiation: Investigation of CG11360 in neuronal development, Field of study: Life Sciences—Developmental Biology (#1842486), University of Oregon, 2019-2022

Adamson Family Award, University of Oregon, 2020

Institute of Neuroscience Scholar Award, University of Oregon, 2019-2021

Outstanding Honors Thesis Award, Indiana University Bloomington, 2019

PUBLICATIONS:

K.H. Fisher, S-L. Lai, C.Q. Doe. Imp and Chinmo are required for embryonic motor neuron axon and dendrite targeting. *Biology Open, accepted*. 2025.

E.A. Bearce, B.T.B. Ricamona, K.H. Fisher, J.R. O'Hara-Smith, D.T. Grimes. Visualization and quantitation of spine deformity in zebrafish models of scoliosis by micro-computed tomography. *STAR Protocols*, Dec 7, 2023. Doi: doi.org/10.1016/j.xpro.2023.102739.

S.E. Mauthner, K.H. Fisher, W.D. Tracey. The *Drosophila* gene *smoke alarm* regulates nociceptor-epidermis interactions and thermal nociception behavior. *bioRxiv* 2021 May. 2021.05.12.44364; doi: doi.org/10.1101/2021.05.12.443649

ACKNOWLEDGMENTS

I would like to first express my gratitude and appreciation to my advisor Dr. Chris Doe. Chris's advisership has helped shape me into a capable and confident scientist and moreover has helped me grow into a confident and strong person in general. Chris was not only a scientific advisor but also as an advisor through an exceptionally challenging time in my life. Without Chris, I would not be writing this dissertation or graduating with my PhD. I will forever be grateful for the support he has given to me and thankful for caring about me as a scientist and also as human being.

I thank the members of the Doe lab (Nathan Anderson, Elena Barth, Ben Brissette, Kasey Drake, Derek Epiney, Josmarie Graciani, Janet Hanawalt, Keiko Hirono, Sen-Lin Lai, Kristen Lee, Laurina Manning, Jordan Munroe, Gonzalo Morales Chaya, Peter Newstein, Heather Pollington, Megan Radler, Matalie Rico Carvajal, Austin Seroka, Rishi Sastry, Alanna Sowles and Chundi Xu) for welcoming me into their group. The Doe lab group is the most positive and nurturing group of people that I have worked with, and every member is willing to help with experiments, writing, and scientific discussion. Many days the Doe lab members uplifted and encouraged me to keep pursing my research and goals.

I would like to thank the members of my committee, Dr. Karen Guillemin, Dr. Judith Eisen, Dr. Tory Herman, and Dr. Matt Smear. I thank them for their support and guidance through my transition into the Doe lab.

Outside of the UO, I would like to thank my long-term mentors Stephanie Mauthner and Rosa Miyares. Stephanie and Rosa encouraged me to continue to pursue research and their influence over the years has helped me grow into a curious and rigorous scientist. I will forever be grateful for their time and dedication to my scientific pursuits. I would not be where I am today without them.

For work in chapter I, I thank Sen-Lin Lai for collaborating on axon targeting and MCFO experiments, as well as help with troubleshooting and discussion. I thank Megan Radler and Josmarie Graciani for assistance with brain dissections. I thank Kristen Lee for helpful discussion on quantification methods.

For work in chapter III, I thank Martin Blum for *Xenopus* data. I also thank my undergrad trainee, Maisey Schering, for help with the generation of guides, injections, and scoring heart defects.

I would like to thank the fly and fish communities for being an excellent source of resources for this work. Specifically, I thank Flybase for their immense resources on the genes studied in this project. I would also like to thank the Zebrafish Information Network (ZFIN) for their resources, specifically annotated expression data that made the L-R patterning screen possible. I extend a special thank you to the Bloomington Drosophila Resource Center (BDSC), located at my undergraduate institution, for providing fly stocks for my project and to the greater fly community. Antibodies from the Developmental Studies Hybridoma Bank (DHSB) were used in this study. I also thank Claude Desplan for providing antibody reagents.

This investigation was supported by HHMI (awarded to Dr. Chris Doe), NIH 5F31HD108945-02 (awarded to Katherine H. Fisher), NSF #1842486 (awarded to Katherine H. Fisher).

DEDICATION

I dedicate this dissertation to my family. To my partner John, who I met in grad school, and who has since been my strongest source of support and encouragement. We have been through so much in this journey and you have always been by my side encouraging me and providing me endless love and support, for taking me to Ducks games, on trips and adventures big and small. I could not have made it through this without you. To my mom and dad, who have always shown up for me, time and time again, and are always available for light-hearted phone calls and laughs. To my sisters and their babies, for providing lightheartedness and fun when I come to visit and for visiting me in Oregon as well. To my dog Buster, who I have lost, you were my first baby and it was such an honor to take care of you and love you. To my reptiles, who inspire my love of science and nature.

TABLE OF CONTENTS

LIST OF FIGURES

CHAPTER I

IMP AND CHINMO ARE REQUIRED FOR EMBRYONIC MOTOR NEURON AXON/DENDRITE TARGETING

Author Contributions

Conceptualization: C.Q.D., K.H.F., S-L.L.; Methodology: K.H.F. S-L.L.; Formal analysis: K.H.F., S-L.L.; Investigation: K.H.F., S-L.L.; Writing – original draft: K.H.F.,C.Q.D; Visualization: K.H.F., S-L.L.; Supervision: C.Q.D.; Project administration: C.Q.D.; Funding acquisition: C.Q.D, K.H.F.

Authors: Katherine H. Fisher, Sen-Lin Lai, and Chris Q Doe

Introduction

The generation of distinct populations of neurons is an essential part of neuronal development. Neurons with diverse function, connectivity, and morphology are important for sensation of and generation of complex behaviors across the animal kingdom. Neural progenitors give rise to distinct populations of neurons throughout development. In both *Drosophila* and mammals, two distinct mechanisms are used to generate neuronal diversity. First, spatial patterning of the neuroectoderm generates molecularly distinct progenitor pools (mammals) or distinct individual progenitors (*Drosophila* neuroblasts, NBs)(Crews 2019; Erclik et al. 2017; Guillemot 2007; A. Sagner and Briscoe 2019). Second, each progenitor undergoes gene expression changes over time, a process called temporal patterning. Temporal patterning occurs in the mammalian spinal cord, cerebral cortex, and retina (Mattar and Cayouette 2015; Andreas Sagner et al. 2021; A. Sagner and Briscoe 2019), and in the Drosophila embryonic ventral nerve cord (VNC; analogous to the vertebrate spinal cord), larval central brain, and optic lobe (Doe 2017; El-Danaf, Rajesh, and Desplan 2023).

In *Drosophila*, temporal patterning occurs via two distinct mechanisms. In the embryonic VNC and optic lobe, a cascade of temporal transcription factors (TTFs) specifies neuronal temporal identity. In the VNC, the cascade is: Hunchback (Hb), Krüppel, Pdm1/2, Castor, and Grainy head (Pollington and Doe 2025). In addition, a TTF cascade occurs within the progeny of central brain Type II NBs, called intermediate neural progenitors (INPs), which sequentially

express the transcription factors Dichaete, Grainy head, and Eyeless over several rounds of cell division (Bayraktar and Doe 2013; Homem et al. 2013; Tang et al. 2022). Finally, distinct TTFs are used in the optic lobe (El-Danaf, Rajesh, and Desplan 2023). In all three regions of the CNS the concept is the same: each TTF in the cascade specifies one or a few specific neuronal and glial cell types.

A second mechanism of temporal patterning occurs in larval central brain neuroblasts, where opposing gradients of two RNA-binding proteins, IGF-II mRNA binding protein (Imp) and Syncrip (Syp), specify different neuronal identities based on the level of each protein (Figure 1)(Guan et al. 2022; Z. Liu et al. 2015). In the mushroom body, Imp and Syp proteins are expressed in opposing gradients that cross-repress each other (Z. Liu et al. 2015). Imp is expressed early in a high-to-low gradient while Syp is expressed late in a low-to-high gradient. Knockout of Imp or Syp results in dramatic loss of early- or late-born mushroom body cell types respectively (Z. Liu et al. 2015). Regulation of translation of the transcription factor Chinmo adds an additional layer of neuronal diversity. Imp positively regulates Chinmo expression, while Syp represses Chinmo expression through binding of the 5'UTR (Z. Liu et al. 2015; Zhu et al. 2006). Furthermore, low levels of Chinmo activate expression of Mamo, creating an additional layer of temporal diversity by generating a intermediate mushroom body cell type (L.-Y. Liu et al. 2019). Similarly, in Type II central brain neuroblasts (Bello et al. 2008; Boone and Doe 2008; Bowman et al. 2008), Imp and Syp are expressed in opposing gradients and Imp is required for early Type II neuron fates, while Syp is required for late-born fates (Ren et al. 2017; Syed, Mark, and Doe 2017). Chinmo is expressed early alongside Imp and both are repressed by

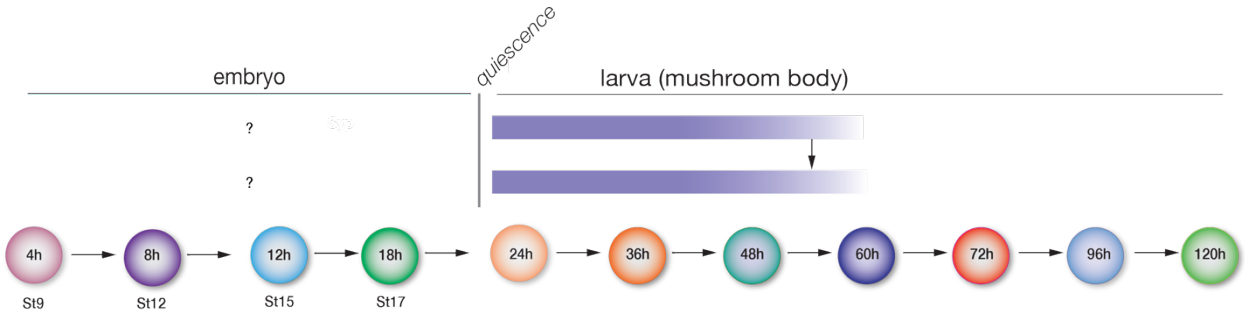

Figure 1. Schematic of known and unknown roles for the larval temporal factors. On the right shows known roles of the indicated larval temporal factors over time; none of these factors has been investigated for a role in the embryonic ventral nerve cord (left). ALH, hours after larval hatching; AEL, hours after egg lay; St, embryonic stage. Timeline not to scale.

Syp midway through larval development (Ren et al. 2017). Two transcription factors E93 and Broad are expressed in the later half of larval development and function to specify late neuronal fates (Ren et al. 2017; Syed, Mark, and Doe 2017).

While the gene regulatory network of these factors has been thoroughly characterized in larvae, little is known about the role of these larval temporal factors -- Imp, Syp, Chinmo, Mamo, Broad, E93 -- in embryonic CNS development. What little is known suggests different mechanisms are used in embryonc versus larval neuroblasts: Castor is a late TTF in the embyonic CNS (Doe 2017), whereas it is an early TTF in larval neuroblasts (Dillon and Doe 2024). Major unknown questions are: Are these larval factors expressed in the embryonic CNS? Do they form opposing Imp/Syp gradients? What is the relationship between the embryonic TTF cascade and Imp/Syp expression? Do they specify neuronal identity, or other aspects of CNS development? Here we address these questions, finding both similarities and differnces in the larval and embryonic Imp/Syp/Chinmo expression and function. Notably, we found that both Imp and Chinmo are required for proper embryonic motor neuron axon targeting to their proper muscle targets, and dendrites mistargeting within the CNS neuropil.

Results

Imp is expressed in a low-high temporal gradient in embryonic neurons

In larval development, Imp is expressed in a high-to-low gradient in neuroblasts, and expression levels are inherited by the daughter cells (Islam and Erclik 2022). However, Imp expression has only been characterized at low resolution and via a GFP knock-in tagged Imp:GFP protein in the embryonic CNS (Adolph et al. 2009). Many open questions remain. Will the larval "late" factors lack embryonic expression? Will the "early" larval Imp gradient continue from embryo to larvae? In general, we want to determine the expression patterns of "late" larval factors in the embryo and test their function. We determined that Imp is expressed globally in the cytoplasm of embryonic neuroblasts (Figure 2A). Imp expression levels are consistent in NBs until stage 12, at which time they show an increase in Imp expression, as quantified in Figure 2B. In post-mitotic neurons, Imp and Chinmo are expressed pan-neuronally (Figure 2C). Imp expression is present throughout embryognesis, while Chinmo expression is detectable in neurons beginning at stage 12. Quantification of early born, mid born, and late born Imp and Chinmo expression showed

that Imp is expressed in a low-to-high gradient, being low in deep, early-born neurons and high in superficial, late-born neurons (Figure 2C-D). Importantly, this is the opposite of the larval

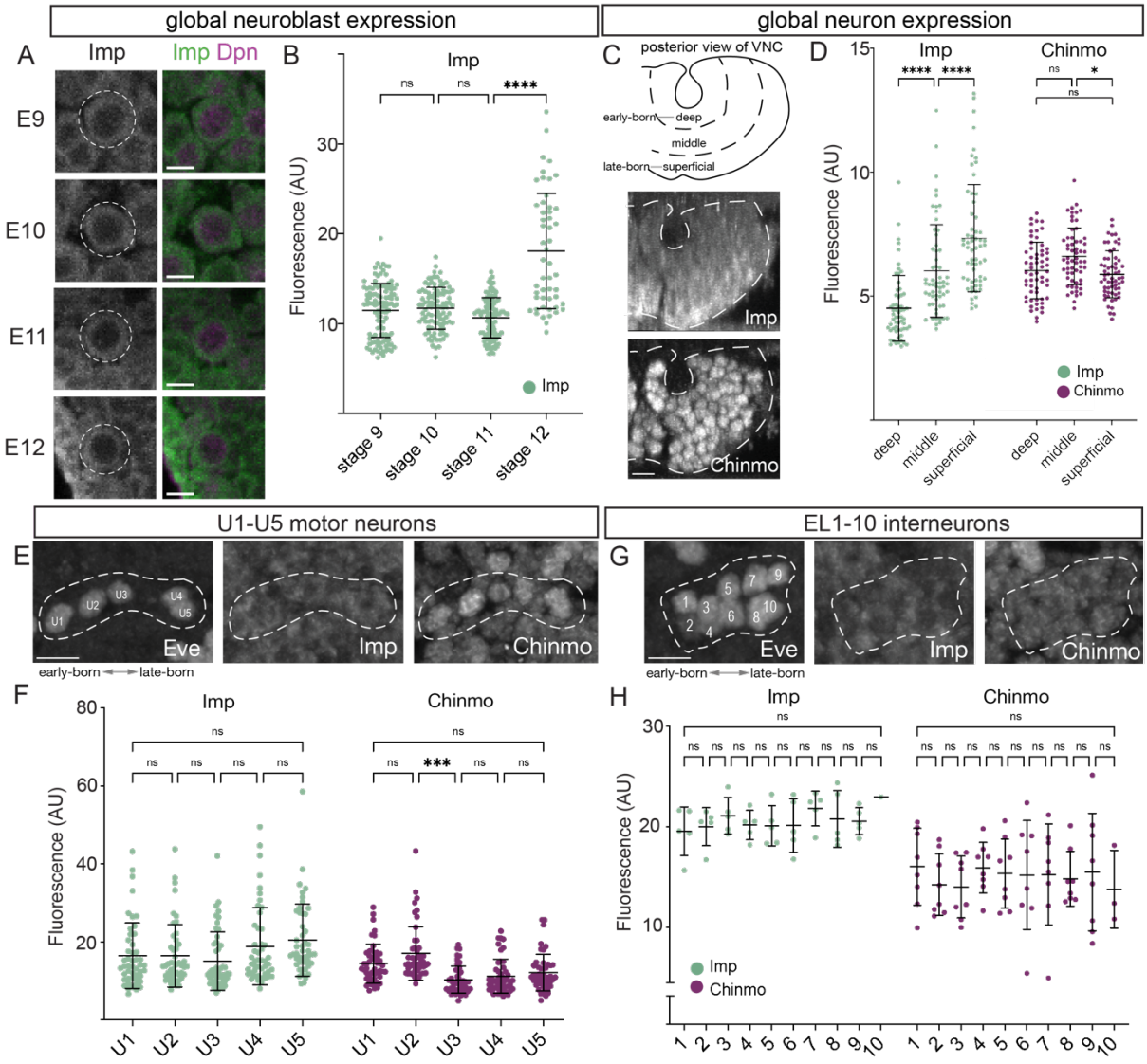

Figure 2. Imp forms a low-to-high gradient in embryos. (A-B) Imp forms a low-to-high gradient in aging embryonic neuroblasts. (A) Imp expression in Dpn+ neuroblasts at the indicated embryonic stages (left). Ventral view. Scale bar = 5μM. (B) Quantification. n > 40 for each stage. (C-D) Imp forms a low-to-high gradient in aging embryonic neurons. (C) Imp and Chinmo expression in a cross-sectional (posterior) view, where older neurons are located in a deep layer and younger neurons are located in a more superficial layer. Chinmo is expressed but not in a gradient. Scale bar = 5μM. (D) Quantification. n > 40 for each stage. (E-F) Imp and Chinmo do not form gradients in the young-old U1-U5 motor neurons, identified by expression of the Eve transcription factor. (E) Imp, Chinmo, and Eve expression in stage 16 embryos. Ventral view. Scale bar = 5μM. (F) Quantification. n > 20 for each neuron. (G-H) Imp and Chinmo do not form gradients in the young-old EL1-EL10 interneurons, identified by lateral expression of the Eve transcription factor. (G) Imp, Chinmo, and Eve expression in stage 16 embryos. Ventral view. Scale bar = 5μM. (H) Quantification. n > 5 for each neuron.

high-to-low gradient. Chinmo expression is relatively uniform across early to late born neurons with variation in expression levels in individual neurons (Figure 2C-D). Broad is expressed in a subset of neurons and has higher expression in thoracic segments; other late factors E93, Mamo, and Syp were not present in embryonic NBs or neurons (Supplemental Figure 1).

To determine if the Imp and Chinmo have similar expression patterns in identified neurons with a known birth-order, we assayed the five U1-U5 from NB7-1; these represent early-born identified neurons (T. Isshiki et al. 2001; Seroka et al. 2020). We found that Imp and Chinmo were both expressed in U1-U5 MNs, but were not distributed in a gradient (Figure 2E-F). We also assayed Imp and Chinmo in the ten Eve lateral neurons (EL1-EL10) from NB3-3 (Tsuji, Hasegawa, and Isshiki 2008; Wreden et al. 2017); these include late-born identified neurons. Imp and Chinmo were both expressed in EL1-EL10 interneurons, but were not distributed in a gradient (Figure 2G-H). Overall, we conclude Imp is expressed in a low-high gradient whereas Chinmo has a more even distribution.

The Imp temporal gradient is not established by the embryonic TTF cascade

To determine if the Imp gradient is generated by the action of the known embryonic TTF cascade (Hb>Kr>Pdm>Cas), we used *en-gal4* to misexpress *UAS-hb* -- which is known to stall the TTF cascade (T. Isshiki et al. 2001; Pollington and Doe 2025; Tran and Doe 2008) and assayed for loss of the Imp gradient. We found that Hb overexpression in the *en-gal4* stripes had no effect on Imp expression in the embryonic CNS (Supplemental Figure 2). We conclude that the TTF cascade is not responsible for generating the observed Imp low to high gradient.

Cross-regulation of Chinmo, Imp, and Syp in the embryonic CNS

Chinmo and Imp show cross-regulation in the larval CNS (Figure 1, right). We wanted to know if these factors show the same or different modes of cross-regulation in the embryonic CNS. In wild type, Chinmo has relatively high expression; Imp has modest expression, and Syp is not detected in neurons, although there is expression in gut cells below the CNS and sporadically in a subset of glia (Figure 3A). In *Imp* mutant embryos, we observed loss of Chinmo expression but we saw no derepression of Syp (Figure 3B, quantified in G). In *chinmo*^{1} mutant embryos, we

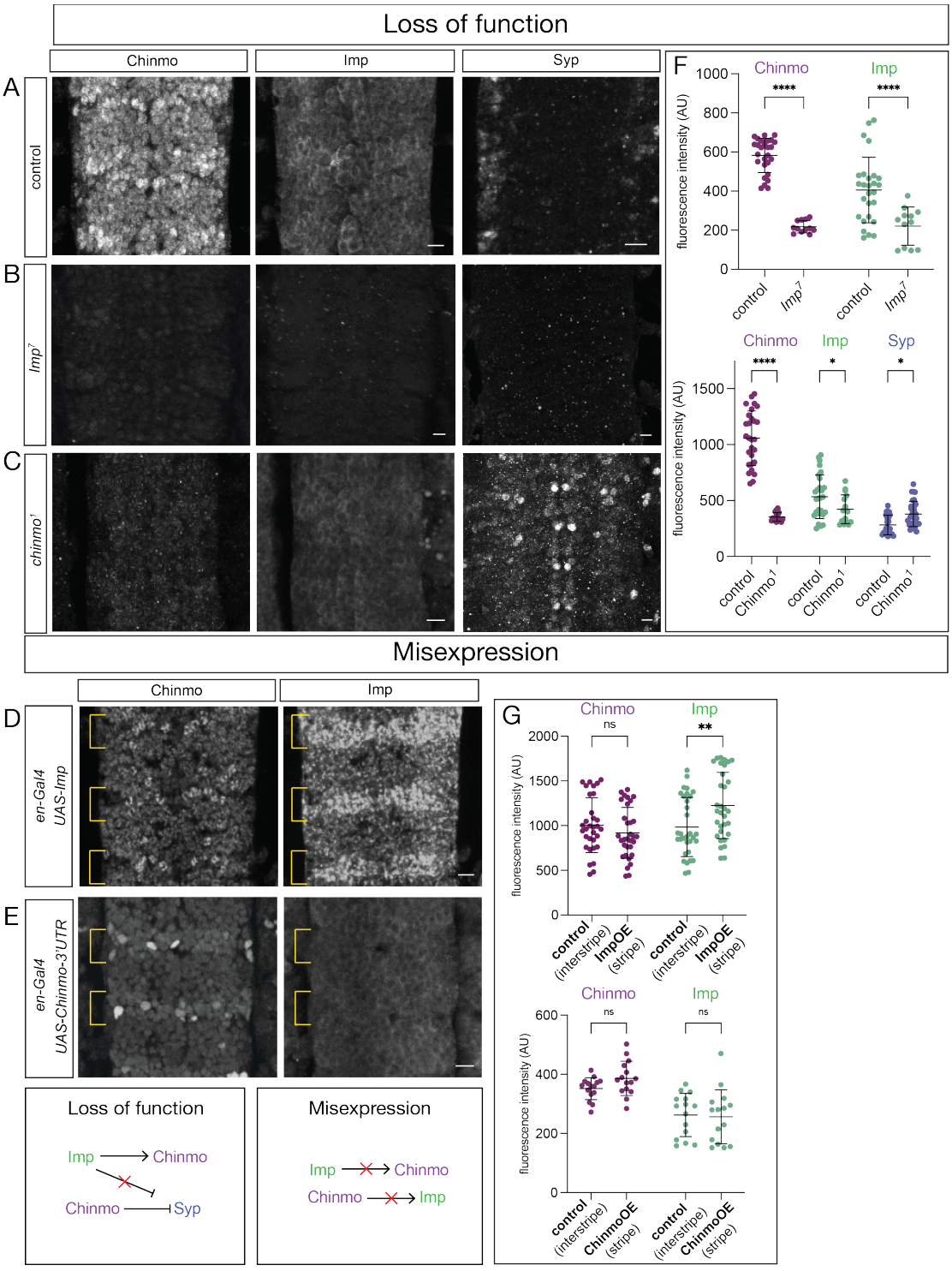

Figure 3. Cross regulation of Imp, Syp and Chinmo in the embryonic VNC. (A) Control stained for Chinmo, Imp, and Syp. (B) *chinmo*^{1} homozygous mutant stained for Chinmo, Imp, and Syp. (C) Chinmo overexpression (*en-gal4 UAS-chinmo*) stained for Chinmo, Imp, and Syp. (D) *Imp*^{7} homozygous mutant stained for Chinmo, Imp, and Syp. (E) Imp overexpression (*en-gal4 UAS-Imp*) stained for Chinmo, Imp, and Syp. (F) Syp overexpression (*en-gal4 UAS-Syp*) stained for Chinmo, Imp, and Syp. All panels show stage 16 embryos, ventral view, scale bar, 5µm. (G) Quantification.

observed loss of Imp expression and de-repression of Syp -- unlike in *chinmo* mutants (Figure 3C, quantified in G). Note that we did not assay *Syp* mutant embryos because there is no expression of Syp in the wild type CNS (Figure 3A). In contrast, overexpression of Imp resulted in no change in Chinmo (Figure 3D, E, quantified in H), despite the overexpression of Imp flattening the Imp gradient (Supplemental Figure 3). Lastly, we assayed overexpression of Chinmo, and found no change in levels of Imp expression (Figure 3F, quantified in 3H). We conclude that (a) there are differences in Chinmo, Imp, and Syp cross-regulation in embryos compared to larval stages; and (b) importantly, loss of Imp and loss of Chinmo had different effects on Syp expression.

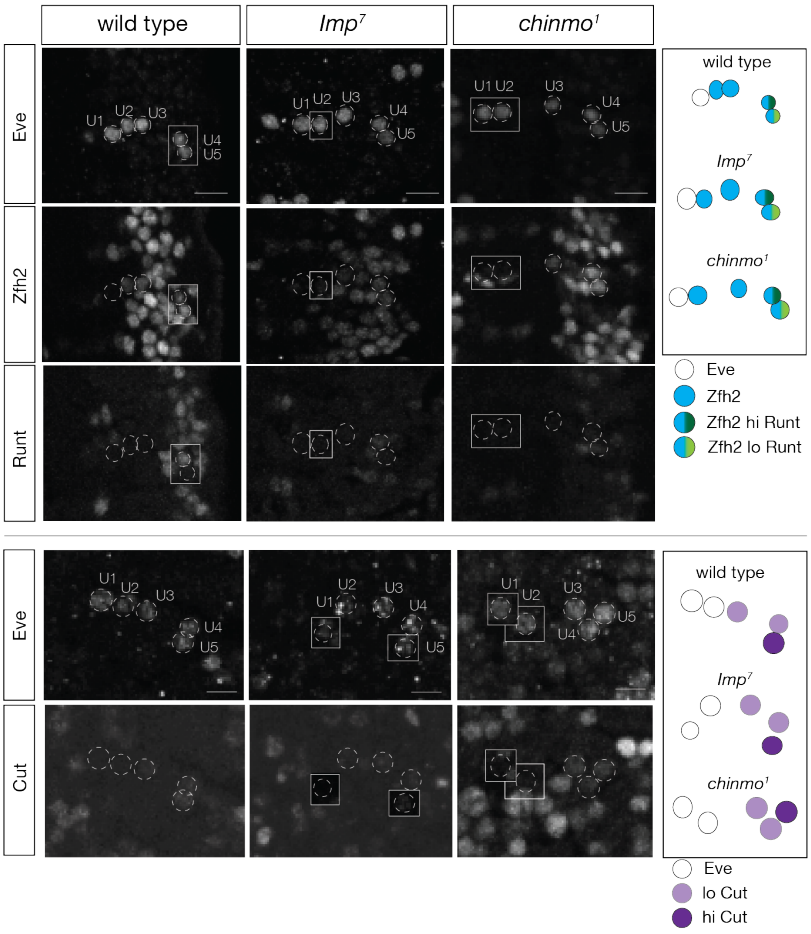

Figure 4. Imp and Chinmo are not required for motor neuron identity
(A) Control; molecular markers show wild type U1-U5 motor neuron identity. Eve, U1-U5; Zfh2, U2 (low), U3-U5; Runt, U4 (high)-U5 (low); Cut (U5). Scale bar = 5µM (B) *Imp*^{7} homozygous mutant; molecular markers show wild type U1-U5 motor neuron identity. Eve, U1-U5; Zfh2, U2-U5; Runt, U4 (high)-U5 (low); Cut (U5). Scale bar = 5µM

Imp does not specify motor neuron molecular identity

To begin our analysis of Imp and Chinmo function in embryos, we assayed their role in motor neuron molecular identity (this section) and motor neuron axon and dendrite targeting (next sections). We chose to analyze the well-characterized U1-U5 motor neurons born from the first five divisions of NB7-1 (Isshiki et al., 2001). In wild type, Eve is expressed in U1-U5, Zfh2 is expressed in U2-U5, Runt is expressed in U4 (high level) and U5 (low level), and Cut is expressed in U5 (Figure 4A). We

observe the same molecular identity in *Imp* and *chinmo* null mutants (Figure 4B). We conclude that loss of Imp has no effect on the molecular identity of the U1-U5 motor neurons.

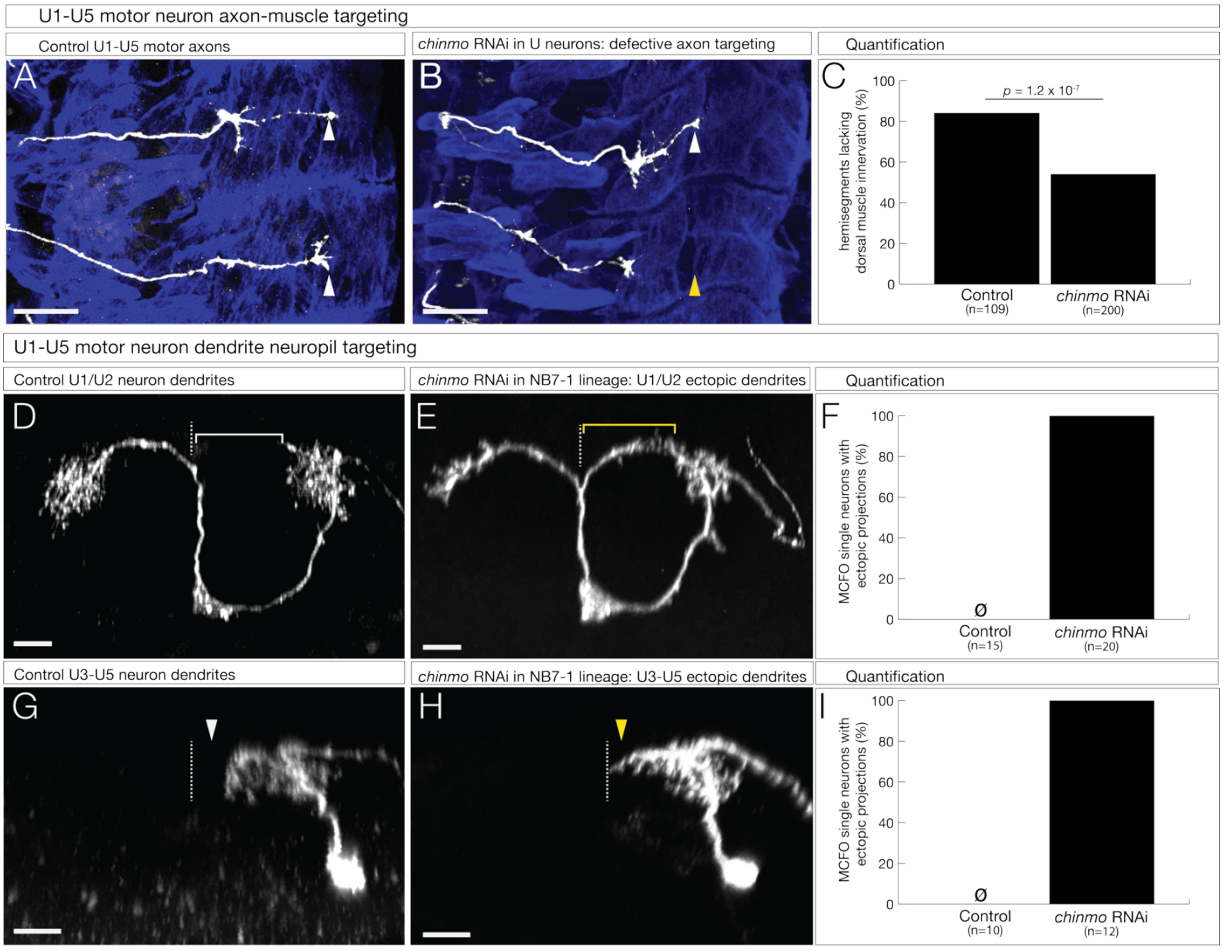

Figure 5. Chinmo is required for motor neuron axon and dendrite targeting
(A-C) Multicolor flip out to obtain single neuron labeling of the U1 or U2 motor neuron dendrites. Posterior view; midline, dashed line. (A) Control U1 or U2 motor neuron assayed in newly hatched larvae. Scale bar, 5 µm. Note lack of midline crossing (white bracket). (B) *chinmo* mutant showing ectopic denrite arbors (yellow bracket) assayed in newly hatched larvae. Scale bar, 5 µm. Note the abnormal midline crossing (yellow bracket). (C) Quantitation. Genetics: NB7-1-KZ-Gal4, R57C10-Flp, UAS-MCFO, UAS-chinmo-RNAi. (D-F) Multicolor flip out to obtain single neuron labeling of the U3-U5 motor neuron dendrites. Posterior view; midline, dashed line. (D) Control U3-U5 motor neuron assayed in newly hatched larvae. Scale bar, 5 µm. Note lack of midline crossing (white arrowhead). (E) *chinmo* mutant showing ectopic denrite arbors contacting or crossing the midline (yellow arrowhead) assayed in newly hatched larvae. Scale bar, 5 µm. (F) Quantitation. Genetics: NB7-1-KZ-Gal4, R57C10-Flp, UAS-MCFO, UAS-chinmo-RNAi assayed in newly hatched larvae. (G-I) U1-U5 motor neurons were labeled with GFP; lateral view, dorsal, up. (G) Controls have extension of motor neurons to the dorsal muscle field. Scale bar, 20 µm. (H) After chinmo RNAi in motor neurons, their axons fail to project to the dorsal muscle field. Scale bar, 20 µm. z(I) Quantitation. Genetics: CQ-gal4, UAS-myrGFP, UAS-chinmo-RNAi, late stage 17.

Chinmo is required for motor neuron axon and dendrite targeting

Chinmo is not required for motor neuron molecular identity, but it may have a role in later events such as axon/dendrite morphogenesis, targeting, or connectivity. We assayed for U1-U5 axon targeting to the dorsal muscle field (U1/U2) or the lateral muscle field (U3-U5). In controls, we observed innervation of both dorsal and lateral muscle fields (Figure 5A; quantified in 5C). In contrast, *chinmo* RNAi expressed in U1-U5 neurons resulted in frequent failure to innervate the dorsal muscles (Figure 5B; quantified in 5C). We conclude that Chinmo is required for proper motor neuron-muscle connectivity.

Next, we used MCFO to specifically label individual U1-U5 motor neurons, and confirmed that control U1/U2 motor neurons were bipolar and had dentritic arbors distant from the midline in newly hatched larvae (Figure 5D; quantified in 5F). In contrast, *chinmo* RNAi expressed in U1-U5 neurons resulted in U1/U2 showing ectopic dendrite projections contacting or crossing the midline in newly hatched larvae (Figure 5D; quantified in 5F). Similar abnormal midline contacting/crossing was observed in the mono-polar U3-U5 motor neurons (Figure 5G,H; quantified in 5I). We conclude that Chinmo is required to prevent ectopic motor neuron dendriting targeting.

Imp is required for motor neuron axon targeting

Imp is also not required for motor neuron molecular identity, but it may have a role in later events such as axon/dendrite morphogenesis, targeting, or connectivity. We assayed for U1-U5 axon targeting to the dorsal muscle field (U1/U2) or the lateral muscle field (U3-U5). In controls, we observed innervation of both dorsal and lateral muscle fields (Figure 6A; quantified in 6C). In contrast, expression of *Imp* RNAi in U1-U5 neurons resulted in frequent failure to innervate the dorsal muscles (Figure 6B; quantified in 6C). We conclude that Imp is required for proper motor neuron-muscle connectivity.

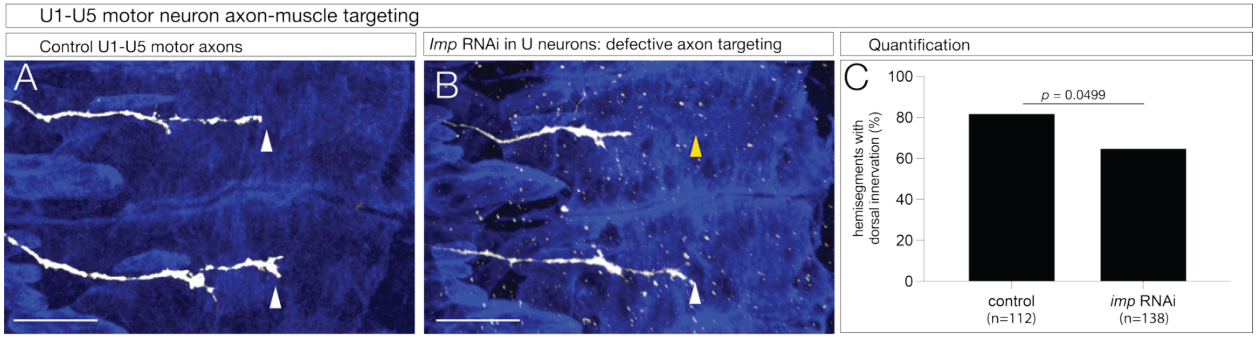

Figure 6. Imp is required for motor neuron axon targeting. (A-C) Multicolor flip out to obtain single neuron labeling of the U1 or U2 motor neuron dendrites. Posterior view; midline, dashed line. (A) Control U1 or U2 motor neuron assayed in newly hatched larvae. Scale bar, 5 µm. (B) *Imp* RNAi in U1-U5 neurons results in ectopic denrite arbors (yellow bracket) assayed in newly hatched larvae. Scale bar, 5 µm. (C) Quantitation. Genetics: NB7-1-KZ-Gal4, R57C10-Flp, UAS-MCFO, UAS-Imp-RNAi.

Discussion

We have found significant differences in the expression, regulation, and function between larval and embryonic stages (Figure 7). We observed the following differences: (1) Whereas larval NBs express opposing gradients of Imp and Syp (Z. Liu et al. 2015), in embryos only Imp is expressed while Syp is undetectable, and thus embryos have no role for Syp. (2) Whereas larval NBs show Imp activating Chinmo but not the opposite (Zhu et al. 2006), in embryos both Imp and Chinmo positively regulate each other. (3) Whereas larval neurons do not show Chinmo repressing Syp (Z. Liu et al. 2015), in embryos Chinmo clearly represses Syp, as *chinmo* mutants de-repress Syp in neurons. (4) Whereas larval NBs show pan-neuronal expression of the mid (Mamo) or late (E93, Broad) temporal factors (Ren et al. 2017; Syed, Mark, and Doe 2017), in embryos Mamo and E93 are not expressed in the CNS, and Broad is only detected in a small subset of neurons.

Knockdown of *chinmo* causes derepression of Syp broadly throughout the embryonic CNS, however knockdown of *Imp* has no effect of Syp levels, consistent with our data showing that Syp is not expressed in the embryonic CNS. Maternal expression of *Imp* in zygotic Imp^{7} mutants may be sufficient to repress Syp, or maternal *Imp* is sufficient to activate sufficient levels of Chinmo to repress *Syp* throughout embryogenesis. The repression of Syp by Chinmo contrasts their relationship in larval development, where Syp represses *chinmo*, and Syp and Imp repress each other (Ren et al. 2017).

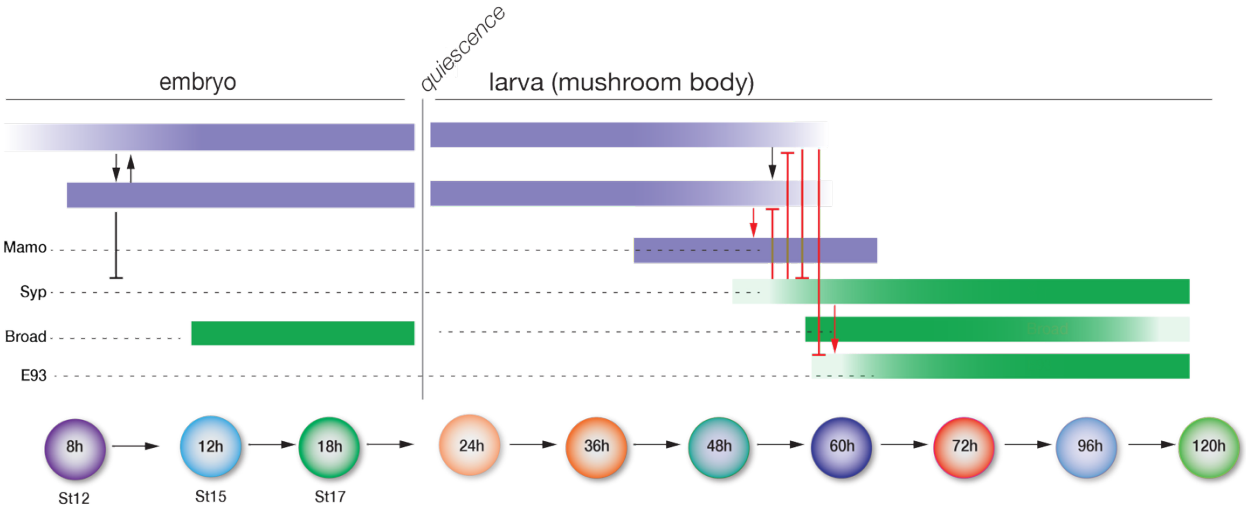

Figure 7. Schematic of embryonic and larval roles of neuronal temporal factors. On the right shows known roles of the indicated larval temporal factors over time; left expression and cross-regulation of the indicated temporal factors in the embryonic VNC. ALH, hours after larval hatching; AEL, hours after egg lay; St, embryonic stage. Timeline not to scale. Arrows, positive regulation; T bars, repressive regulation. Broad* indicates scattered neuronal expression; not pan-neuronal.

Previous work has shown that *Imp* is required in larvae for Kenyon cell specification: knockdown of *Imp* or *Syp* alters the ratio of early-born vs late-born neuronal identity (Hamid et al. 2024; Z. Liu et al. 2015), in contrast, *Imp* and *chinmo* have no role in motor neuron specification, but rather they are both required in post-mitotic motor neurons for axon targeting to the correct body wall muscle. Similarly, Chinmo knock down in the NB7-1 lineage results in mis-targeting of motor neuron dendrites within the CNS neuropil. Unfortunately we were unable to test for a similar role of Imp in motor dendrites, as we were unable to generate MCFO-labeled neurons, perhaps due to Imp triggering NB7-1 apoptosis (Guan et al. 2022; Samuels et al. 2020). Similarly, at larval stages, loss of *Imp* does not alter expression of pMad, a marker of motor neurons (Boylan et al. 2008), suggesting that *Imp* is also dispensable in larvae for specification of motor neuron identity. Imp is an RNA-binding protein, and its RNA cargo have been defined in larval neuroblasts, where Imp plays a role in regulation of proliferation (Samuels et al. 2020; Yang et al. 2017); these RNAs are also good candidates for a role in embryonic dendrite and axon targeting.

Chinmo is required for generation of distinct cell types in larval mushroom body neurons (Z. Liu et al. 2015; Zhu et al. 2006). In contrast, we found that Chinmo is dispensable for neuronal identity, in U1-U5 motor neurons, but is required for motor neuron axon targeting and

targeting of motor neuron dendrites. Interestingly, Syp is required in larval motor neurons where *syp*, along with *msp300*, is required for new synapse formation. Additionally, *syp* is required for synaptic plasticity in motor neurons (Titlow et al. 2020). Interestingly, we found that Chinmo is required to repress Syp expression in the embryonic CNS. Deprepression of Syp in *chinmo*^{1} mutants may promote additional synapse formation or synaptic plasticity in motor neuron dendrites leading to ectopic neurite formation.

There is a major difference in time scale between embryonic and larval neurogenesis: embryonic neurogenesis is completed in less than one day, whereas larval neurogenesis lasts 5 days. The shorter time of embryonic neurogenesis may requre a more "hard-wired" mechanism such a TTF cascade that switches TTF expression approximately every hour (Pollington, Seroka, and Doe 2023), whereas longer larval neurogenesis may provide time to generate and respond to gradients of Imp and Syp RNA-binding proteins (Islam and Erclik 2022). We found that overexpression of Hb in NBs, which stalls the TTF cascade and prolongs Hb expression (T. Isshiki et al. 2001) does not alter the Imp gradient in post-mitotic neurons. Additionally, overexpression of Imp, creating levels similar to Imp expression in late-born neurons, does not alter Hb expression in NBs. These results suggest that Imp/Chinmo and the TTF cascade function in separate pathways to guide neuronal development; the TTF cascade is required for cell type identity and Imp/Chinmo are required for neurite targeting and morphology in embryonic development.

In larval development, Imp regulates proliferation of neuroblasts through binding to *myc* mRNA (Samuels et al. 2020). The scarcity of ImpRNAi MCFO clones suggests that *Imp* may be required for NB survival and proliferation. We did not see evidence of NB loss in *Imp*^{7}, however maternal *Imp* transcripts may be sufficient to prevent loss of NBs. Thus, our results show that Imp expression in NBs may be important for survival of NBs in the embryo, although further work needs to be done to confirm this role.

Our finding that Imp and Chinmo both show failure of motor axons to target their correct body wall muscle target is similar to the *Imp* mutant phenotype described for larval motor neurons, where reduced Imp led to reduced motor neuron bouton number at the neuromuscular junction (Boylan et al. 2008). Previous work imaging movement of Imp:GFP in motor axons showed that Imp is trafficked bidirectionally (Boylan et al. 2008); this movement may be defective in *Imp* mutants and explain the reduced bouton formation in larval motor neurons. It

seems likely that Imp is also moving bidirectionally in embryonic motor neurons; this would be an interesting question to explore in the future.

Methods

Antibody staining

For embryonic CNS imaging, embryos were transferred from apple caps into collection baskets and rinsed with dH_2O. Embryos were dechorionated in 100% bleach (Clorox, Oakland, CA) for 4min with gentle agitation. Dechorionated embryos were rinsed with dH_2O for 30sec. Embryos were fixed 20mins in 2mL Eppendorf tubes containing equal volumes of heptane (Fisher Chemical, Eugene, OR, H3505K-4) and 4% PFA diluted in PEM [100mM PIPES pH6.95 (Sigma, St. Louis, MO), 2mM EDTA pH8.0 (Sigma, St. Louis, MO) and 1mM $MgSO_4$ (Sigma, St. Louis, MO). The lower fix layer was removed, and an equal volume of methanol was added to each tube. Tubes were then subject to vigorous agitation for 1 min in a step required for removing the vitelline membrane. Nearly all liquid was removed from the tubes, leaving the embryos. Embryos were rinsed in Methanol (Fisher Chemical, Eugene, OR, Lot# 206197, Cat. A412P-4) three times and stored at -20°C. Embryos were washed three times for 5 minutes with rocking in 0.1% PBST (1xPBS/0.1% Triton-x 100). PBST was removed and embryos were blocked with 5% normal donkey serum (Jackson ImmunoResearch Laboratories, Inc., West Grove, PA) in PBST for 30 min at room temp with rocking. PBST was removed and antibody mixes in PBST were added and rocked overnight at 4°C. Primary antibody mixes were removed and embryos were washed for >15 minutes three times in PBST with rocking. PBST was removed and secondary antibody diluted in PBST was added. Embryos were rocked at room temperature for 2 hours or rocked overnight at 4°C. Embryos were washed for >15 minutes three times in PBST with rocking.

After washing off secondary, embryos were washed three times in PBS then mounted in lysine coverslips and dehydrated in an ethanol series (30%, 50%, 70%, 90%, 100%). Embryos were washed an additional time in 100% ethanol. Next, embryos were washed two times in xylenes (Sigma, St. Louis, MO), then mounted in DPX mounting media (Sigma, St. Louis, MO) and dried at room temperature for two days before imaging.

For imaging axon targeting to muscles, embryos were transferred into 50% glycerol for 20 minutes or until embryos have settled at the bottom of the tube. The 50% glycerol was removed, and 90% glycerol was added. Embryos were left at room temperature overnight to let them fully settle to the bottom of the tube before imaging.

For MCFO analysis of dendrite targeting, embryos that were *UAS-MCFO*, *UAS-ImpRNAi* or *chinmo-RNAi*, *CQ2-gal4* were collected over a 24-hour window then aged for 24 hours. Freshly hatched larval brains were dissected in HL3.1 (Feng, Ueda, and Wu 2004), fixed in 4% paraformaldehyde, and mounted on lysine coverslips. Brains were immunostained on coverslips as described above. Note that *UAS-chinmoRNAi* experiments generated ~3 hemisegments with labeled motor neurons, whereas *UAS-ImpRNAi* experiments generated a single labeled neuron in over 40 brains; why this genotype gave such a low number of labeled neurons despite identical treatment of chinmo RNAi and Imp RNAi is unknown.

For MCFO analysis of axon targeting, embryos that were *UAS-MCFO*, *UAS-ImpRNAi* or *chinmo-RNAi*, *NB7-1-gal4* were collected over a 24-hour window then fixed in 4% paraformaldehyde, and stage 17 embryos were immunostained on coverslips as described above.

Primary and secondary antibodies

Primary antibodies used were: chicken anti-GFP, 1:1000 (Aves Labs, Davis, CA); rabbit anti-Imp 1:500 (MacDonald lab, UT Austin); rabbit anti-Syp 1:1000 Desplan Lab, NYU); rat anti-Deadpan 1:20 (Abcam, Eugene, OR); mouse anti-Hunchback 1:200 (Abcam, Eugene, OR); mouse anti-Eve 1:100 (DSHB, Iowa City, Iowa); guinea pig anti-Chinmo 1:200 (Desplan Lab, NYU); rat anti-Zfh2 1:250 (Doe Lab); mouse anti-Broad 1:20 DSHB, Iowa City, Iowa; guinea pig anti-Mamo 1:200 (Desplan Lab, NYU); guinea pig anti-E93 1:500 (Doe lab); mouse anti-En, 5mg/mL (DSHB, Iowa City, Iowa); mouse anti-Eve[2B8], 5mg/mL, (DSHB, Iowa City, Iowa); rabbit anti-Eve, 1:250 (Doe lab); rabbit anti-Hb, 1:200 (Tran and Doe 2008); guinea pig anti-Runt, 1:1000 (Sullivan, Warren, and Doe 2019); rat anti-Tm1[MAC141], 1:500 (Abcam, Waltham, MA, USA); mouse anti-HA (Biolegend [901513]); chicken anti-V5 (Bethyl [A190-218A]); rat anti-Flag (Novus [NBP1-06712]); rat anti-Ollas Novus [NBP1-06713])

Secondary antibodies used were: DyLight 405, AlexaFluor 488, rhodamine Red™-X, AlexaFluor 555, or Alexa Fluor 647-conjugated AffiniPure™ donkey anti-IgG (Jackson

ImmunoResearch, West Grove, PA, USA). The samples were mounted in 90% glycerol with Vectashield (Vector Laboratories, Burlingame, CA) or DPX (Sigma, St. Louis, MO).

Confocal Microscopy

Images were captured with a Zeiss LSM800, LSM 900 or LSM 900-Airyscan2 laser scanning confocal microscope with a z-resolution of 0.25 μm (Carl Zeiss AG, Oberkochen, Germany) equipped with an Axio Imager.Z2 microscope. A 40x/1.40 NA Oil Plan-Apochromat DIC m27 objective lens and a 63x/1.40 Oil Plan-Apochromat DIC m27 objective lens and GaAsP photomultiplier tubes were used. Software program was Zen 2.3 (blue edition) (Carl Zeiss AG, Oberkochen, Germany). Images were processed using the open-source software FIJI or Imaris (Oxford Instruments plc, UK). Figures were assembled in Adobe Illustrator (Adobe, San Jose, CA). For each independent experiment, all samples were acquired using identical acquisition parameters.

Motor neuron axon and dendrite imaging

Genetics for Figure 5 and 6. Dendrite: *NB7-1-KZ, R57C10-Flp, UAS-MCFO* with *UAS-LacZ* for controls or *UAS-chinmo-RNAi* or *UAS-Imp-RNAi* for experimental groups. Axon: *CQ-gal4, UAS-myrGFP*, with *UAS-LacZ* for controls or *UAS-chinmo-RNAi* or *UAS-Imp-RNAi* for experimental groups. Embryo staging was done according to gut morphology, ensuring that both controls and experimentals were at the same age (late stage 17).

Statistical analyses

Statistics were computed using Prism (GraphPad, Boston, MA). All statistical tests used are listed in the figure legends. P-values are reported in the figures. n.s. = not significant, where $p>0.05$. Plots were generated using Prism (GraphPad).

Figure production

Images for figures were processed in FIJI. Figures were assembled in Adobe Illustrator (Adobe, San Jose, CA). Any changes in brightness or contrast were applied to the entire image.

CHAPTER II

CONTRIBUTION OF SEQUOIA TO EMBRYONIC NEUROBLAST AND NEURON PATTERNING AND MORPHOLOGY

Author Contributions

Conceptualization: C.Q.D., S-L.L.; Methodology: K.H.F.; Formal analysis: K.H.F.; Investigation: K.H.F., S-L.L.; Writing – original draft: K.H.F.; Visualization: K.H.F.; Supervision: C.Q.D.; Project administration: C.Q.D.; Funding acquisition: C.Q.D, K.H.F.

Authors: Katherine H. Fisher, Sen-Lin Lai, Chris Q. Doe

Introduction

The nervous system contains a multitude of specialized neuronal cell types that are critical for forming functional neuronal circuits. A single neuronal progenitor generates many differing cell types over time. In the *drosophila* embryo, sequential expression of transcription factors over time divides neurons into different temporal cohorts, with early born cells expression one set of transcription factors, and late born cells expressing a differing set of transcription factors (Takako Isshiki et al. 2001). Expression of this temporal transcription factor (TTF) cascade not only generates neuronal diversity but may also influence synaptic specificity and axonal innervation. Neurons have been shown to target their synapses in small domains with other neurons from the same temporal cohorts (Takako Isshiki et al. 2001; Mark et al. 2021). The mechanisms controlling synaptic specificity in the central nervous system (CNS) are not well understood. Does the TTF cascade solely control synaptic targeting domains or are other neuronally expressed factors involved?

The pan-neuronally expressed gene, *sequoia,* is a candidate gene that may function in neuronal morphology and synaptic specificity. In the *Drosophila* retina, Sequoia is expressed in a gradient in photoreceptor cells, and this gradient is required for axons to project into the proper layer (Petrovic and Hummel 2008). Loss of *sequoia* results in multiple axons targeting to the same layer. Additionally, *sequoia* functions in *Drosophila* sensory neurons in the peripheral nervous system, called multidendritic (md) neurons, to regulate dendrite and axon morphogenesis. Loss of *sequoia* results in over-branching of dendrites in md neurons, but shortened axon projections (Brenman et al. 2001; Grueber, Jan, and Jan 2002).

We hypothesized that *sequoia* may function in the embryonic CNS to control neuronal morphology. Here we use the *Drosophila* embryo, specifically the NB 7-1 lineage, to determine how *sequoia* functions in synaptic patterning and tiling in motor neurons of the CNS. Key questions we address are: Is there a *seq* gradient in the embryonic CNS, and does this affect neuron morphology? Does *seq* interact with the TTF cascade?

Results

Sequoia is expressed in a low-to-high gradient in the embryonic CNS

To determine if Sequoia is expressed in a gradient, we quantified pixel intensity of *sequoia::GFP* expression in neuroblasts from stage 9-12 of embryonic development. We validated that the *sequoia::GFP* line recapitulates Sequoia protein expression by staining with both GFP and a Sequoia antibody (data not shown). Sequoia expression is relatively uniform across neuroblasts, with a slight peak at stage 10 (Figure 1A-A'). Quantification of Sequoia in early-born Hunchback(Hb)+ cells and late-born Castor(Cas)+ cells showed that Sequoia expression in lower in early born cells, and higher in late born cells (Figure 1B-B'). Finally, quantifying Sequoia expression in the U motor neurons (UMNs) produced from the 7-1 lineage showed a low-to-high gradient of Seq over U1-U5 (Figure 1C-C'). These data confirm that Sequoia is expressed in a low-to-high gradient across neurons in the embryonic CNS both globally and in a specific lineage of sequentially born cells.

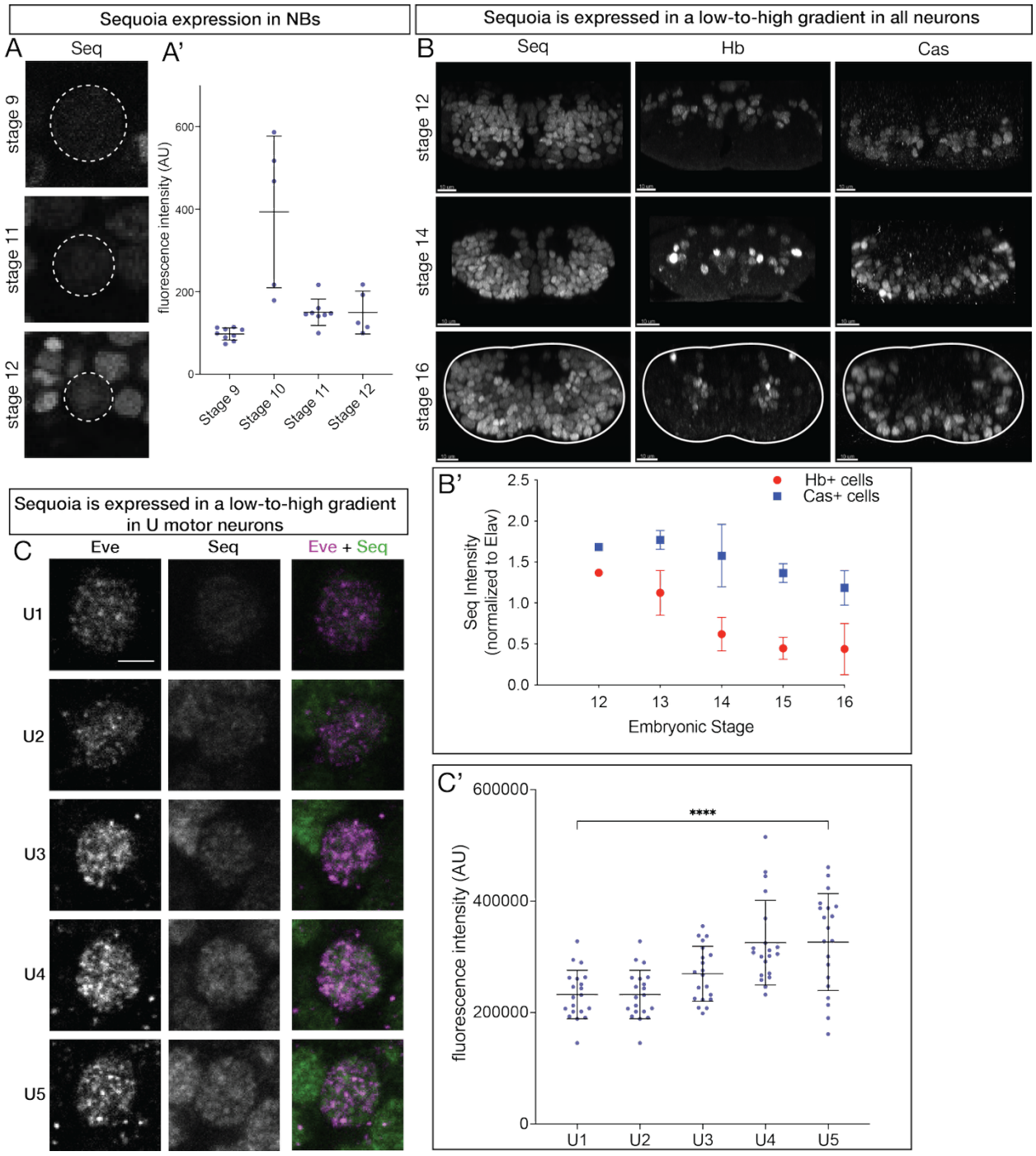

Figure 1. Sequoia is expressed in a low-to-high gradient. A) Sequoia expression in neuroblast at embryonic stage 9, 11, and 12. A') Quantitation of Sequoia protein expression with a peak at stage 10. B) Sequoia expression in early-born Hb+ and late-born Cas+ cells across embryonic development from stage 12-16. B') quantitation of Sequoia in Hb+ and late-born Cas+ cells. Sequoia expression is higher in late-born Cas+ cells than in early-born Hb+ cells at all quantified time points. C) Sequoia expression in UMNs from the 7-1 NB lineage. C') Quantitation of Sequoia in U1-U5. Highest expression is seen in late-born U5 neurons.

The Sequoia gradient does not interact with the TTF cascade

To determine if the Sequoia gradient interacts with the temporal transcription factor cascade, we overexpressed Sequoia in the UMNs and assessed TTF expression. Overexpression of Sequoia had no effect on the expression of Hb, Kr, or Cas (Figure 2). Normal expression of Hb was observed in U1-U2, Kr expression in U1-U3, and Cas expression in U5 at embryonic stage 16.

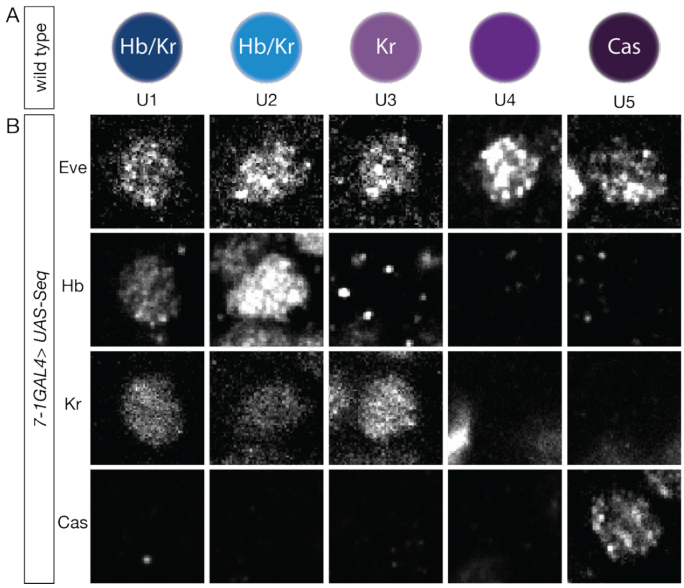

Figure 2. The Sequoia gradient acts independent from the TTF cascade. A) In wild type embryos, U1-U2 express Hb and Kr, U3 expressed Kr, and U5 expressed Cas. B) Overexpression of Sequoia in UMNs does not change the TTF expression profile of these neurons.

Sequoia is not required for motor neuron axon targeting

Graded Sequoia expression is required in photoreceptor cells to properly pattern axons. We hypothesized that the Sequoia gradient in embryos may play a similar role. To test whether the Sequoia gradient affects neuronal morphology, we overexpressed *sequoia* in NB7-1 (7-1GAL4 *UAS-seq*) to flatten the gradient in UMNs and assessed axon targeting. UMN axons target to specific muscles in the larval body wall and targeting is largely completed by the last stage of embryogenesis. Embryos showed no evidence of aberrant axon targeting (Figure 3). Further, we filleted third instar larvae to assess morphology of mature neuromuscular junctions and saw no obvious defects in NMJ morphology (Figure 3, scale bar 20µm).

Discussion

We observed that overexpression of *sequoia* in the neuroblast had no effect on the TTF cascade in NB7-1 progeny. This suggests that Sequoia expression levels have no effect on the expression

of the TTF cascade. It would be interesting to alter the TTF cascade, through overexpression of Hb, to see if the Sequoia gradient is established by the sequential expression of the TTF cascade.

As overexpression of Sequoia in NB7-1 did not alter the number of UMNs, we hypothesize that the Sequoia gradient is not dependent on the TTF cascade. If the TTF cascade is not required to establish the Sequoia gradient, then this may suggest that Sequoia is acting independent from the TTF cascade, and potentially as a regulator of synaptic or dendritic targeting rather than specifying cell identity. While no gross morphology differences in NMJs were observed with *sequoia* overexpression, further analysis of synapse number and morphology may reveal a more specific role for *sequoia* in motor neurons.

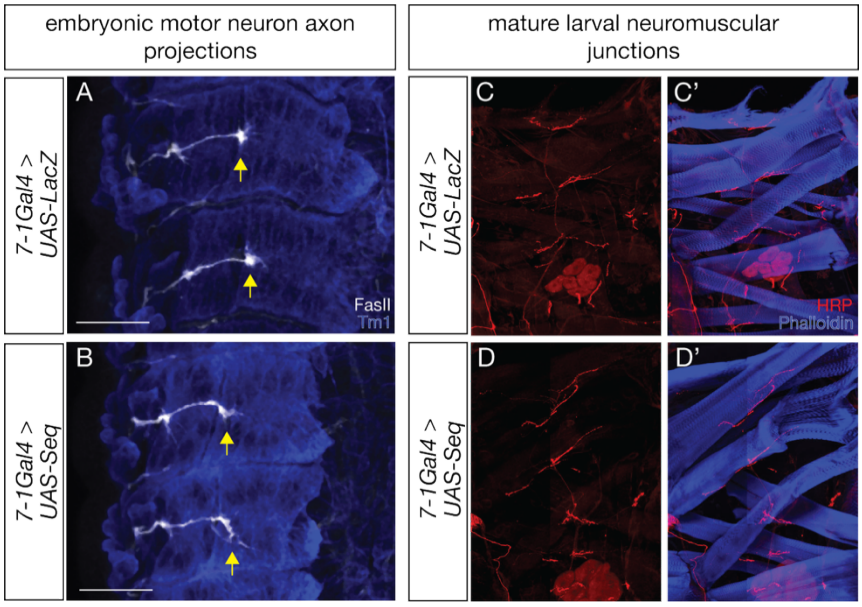

Figure 3. Sequoia overexpression is not sufficient to induce axonal phenotypes. A) Axon targeting of 7-1 UMNs labeled with FasII and targeting to dorsal muscle (Tm1) in late stage 17 embryos. WT axons extend to dorsal muscle 9. B) Overexpression of Seq results in axon targeting to muscle 9 similar to WT. scale bar = 20µm. C) WT NMJ labeled with HRP, C') overlay with muscle cells (phalloidin). D) overexpression of *seq* does not affect morphology of the NMJ D') overlay with muscle cells.

Sequoia has been shown to be a negative regulator of md sensory neuron dendrites and a positive regulator of axon outgrowth in md neurons (Brenman et al. 2001; Grueber, Jan, and Jan 2002). We did not see an effect of overexpression of Sequoia in motor neuron axons, but it is possible that the targeting of the dendrites to the neuropil may be affected. Further overexpression and loss-of-function experiments aimed at exploring dendritic tiling is needed to determine if Sequoia plays a role in dendrite growth outside of the PNS.

Methods

Fly stocks

Stock	Source or reference	Identifier
w; UAS-seq	BDSC	RRID:BDSC_9244
w; UAS-LacZ	BDSC	RRID:BDSC_8529
w; CQ2-Gal4	BDSC	RRID:BDSC_7466
NB7-1-KZ	Doe lab	N/A
yw; seq::GFP	BDSC	RRID:BDSC_92639

Antibody staining

For embryonic CNS imaging, embryos were transferred from apple caps into collection baskets and rinsed with dH_2O. Embryos were dechorionated in 100% bleach (Clorox, Oakland, CA) for 4min with gentle agitation. Dechorionated embryos were rinsed with dH_2O for 30sec. Embryos were fixed 20mins in 2mL Eppendorf tubes containing equal volumes of heptane (Fisher Chemical, Eugene, OR, H3505K-4) and 4% PFA diluted in PEM [100mM PIPES pH6.95 (Sigma, St. Louis, MO), 2mM EDTA pH8.0 (Sigma, St. Louis, MO) and 1mM $MgSO_4$ (Sigma, St. Louis, MO). The lower fix layer was removed, and an equal volume of methanol was added to each tube. Tubes were then subject to vigorous agitation for 1 min in a step required for removing the vitelline membrane. Nearly all liquid was removed from the tubes, leaving the embryos. Embryos were rinsed in Methanol (Fisher Chemical, Eugene, OR, Lot# 206197, Cat. A412P-4) three times and stored at -20°C. Embryos were washed three times for 5 minutes with rocking in 0.1% PBST (1xPBS/0.1% Triton-x 100). PBST was removed and embryos were blocked with 5% normal donkey serum (Jackson ImmunoResearch Laboratories, Inc., West Grove, PA) in PBST for 30 min at room temp with rocking. PBST was removed and antibody mixes in PBST were added and rocked overnight at 4°C. Primary antibody mixes were removed and embryos were washed for >15 minutes three times in PBST with rocking. PBST was removed and secondary antibody diluted in PBST was added. Embryos were rocked at room temperature for 2 hours or rocked overnight at 4°C. Embryos were washed for >15 minutes three times in PBST with rocking.

Embryos were transferred into 50% glycerol for 20 minutes or until embryos have settled at the bottom of the tube. The 50% glycerol was removed, and 90% glycerol was added.

Embryos were left at room temperature overnight to let them fully settle to the bottom of the tube before imaging.

Larval Fillets

Third instar wandering larvae were picked from crosses with a paintbrush and transferred into HL3.1(Feung *et al*., 2004). The cuticle was cut and pinned down to create a flat piece of cuticle and fixed in 4% paraformaldehyde. Fillets were washed in 0.2% PBST three times and then stained with primary and secondary antibodies. Samples were mounted in vectashield.

Primary and secondary antibodies

Primary antibodies used were: chicken anti-GFP, 1:1000 (Aves Labs, Davis, CA); rat anti-Deadpan 1:20 (Abcam, Eugene, OR); mouse anti-Hunchback 1:200 (Abcam, Eugene, OR); rabbit anti-Castor 1:1000 (W. Odenwald Lab); mouse anti-Eve[2B8], 5mg/mL, (DSHB, Iowa City, Iowa); rabbit anti-Eve, 1:250 (Doe lab); rat anti-Tm1[MAC141],

Secondary antibodies used were: DyLight 405, AlexaFluor 488, rhodamine Red™-X, AlexaFluor 555, or Alexa Fluor 647-conjugated AffiniPure™ donkey anti-IgG (Jackson ImmunoResearch, West Grove, PA, USA). The samples were mounted in 90% glycerol with Vectashield (Vector Laboratories, Burlingame, CA).

Confocal Microscopy

Images were captured with a Zeiss LSM800 or LSM 710 (Carl Zeiss AG, Oberkochen, Germany) equipped with an Axio Imager.Z2 microscope. A 40x/1.40 NA Oil Plan-Apochromat DIC m27 objective lens and a 63x/1.40 Oil Plan-Apochromat DIC m27 objective lens and GaAsP photomultiplier tubes were used. Software program was Zen 2.3 (blue edition) (Carl Zeiss AG, Oberkochen, Germany). Images were processed using the open-source software FIJI or Imaris (Oxford Instruments plc, UK). Figures were assembled in Adobe Illustrator (Adobe, San Jose, CA). For each independent experiment, all samples were acquired using identical acquisition parameters.

Statistical analyses

Statistics were computed using Prism (GraphPad, Boston, MA). All statistical tests used are listed in the figure legends. *<0.0332, **<0.0021, ***<0.0002, otherwise P-values are reported in the figures. n.s. = not significant, where p>0.05. Plots were generated using Prism (GraphPad).

Figure production

Images for figures were processed in FIJI. Figures were assembled in Adobe Illustrator (Adobe, San Jose, CA). Any changes in brightness or contrast were applied to the entire image.

BRIDGE

In chapters I and II, I established the gene regulatory network of the temporally expressed RNA-binding proteins and transcription factors in *drosophila* motor neuron development.

In the following chapter, I investigate another gene regulatory network controlling left-right patterning. This project, while conducted on a different signaling pathway, draws on the same principle of gene regulation and cell-cell signaling to achieve a target morphology.

CHAPTER III

GENETIC DISSECTION OF FLUID FLOW SIGNALING IN LEFT-RIGHT PATTERNING OF ZEBRAFISH

Author Contributions

Conceptualization: D.T.G., K.H.F.; Methodology: K.H.F., M.B.; Formal analysis: K.H.F.; Investigation: Figure 2: K.H.F., M.S.; Figure 3 & 4: M.B.; Writing – original draft: K.H.F.; Visualization: K.H.F., M.B.; Supervision: D.T.G.; Project administration: D.T.G.; Funding acquisition: D.T.G., K.H.F.

Author List: Katherine H. Fisher, Maisey Schering, Martin Blum, Daniel T. Grimes

Introduction

Cell-cell communication is crucial for patterning and morphogenesis. One mechanism of communication relies on extracellular fluid flows. Flows play critical roles in the kidney, vasculature, reproductive tracts, brain ventricles, and spinal canal (Freund et al. 2012). Aberrant flows cause developmental diseases including congenital heart disease (CHD) (Hoffman and Kaplan 2002), heterotaxy (Sutherland and Ware 2009), and hydrocephalus (Kothari 2014). Compared to chemical signaling pathways like Wnt or Hh, flow-induced pathways, including how flow signals are sent, sensed, and transduced, are poorly understood. Identifying new regulators of flow signaling and dissecting how they work will give insight into diseases caused by aberrant flow.

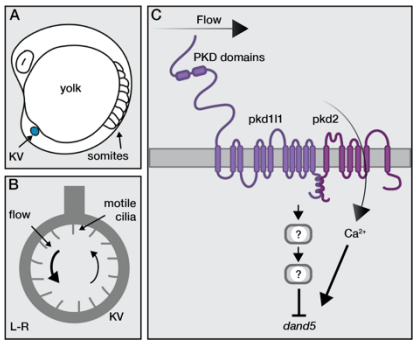

Fig 1. The L-R patterning system in zebrafish. A) Symmetry is broken in Kupffer's vesicle (KV). **B)** Asymmetric flow is generated by motile cilia in KV. **C)** Model of the flow sensory pathway, where Pkd1l1 and Pkd2 sense and transduce flow resulting in *dand5* repression.

The tractable left-right (L-R) patterning system in zebrafish (Grimes and Burdine 2017; Matsui and Bessho 2012) is an ideal model for identifying components of the flow sensory pathway (**Figure 1**). In early embryonic development, asymmetric fluid flow in the zebrafish L-R organizer, called Kupffer's vesicle (KV), breaks L-R symmetry (Kramer-Zucker et al. 2005; Nonaka et al. 2002) (**Figure 1A**). KV is a transient spherical structure made of cells with motile cilia that

generate fluid flow (Essner et al. 2005) (**Figure 1B**). Flow is stronger on the left side than the right. Cells in KV sense this asymmetric flow signal, which results in post-transcriptional repression of *dand5* mRNA, the target of the flow signal, on the left side only (Hojo et al. 2007; Schweickert et al. 2010). It is hypothesized that the motile cilia in KV act as mechanosensory organelles to detect flow signals (McGrath et al. 2003; Shinohara and Hamada 2017; Yoshiba et al. 2012). In other left-right organizers, such as in mice and the African-clawed frog, specific cells on either side of the organizer, called sensory cells, contain non-motile cilia that are required for fluid flow detection (Schweickert et al. 2010). Additionally, the cytoskeleton also plays a role in symmetry breaking by creating subcellular chiral structures that influence laterality (McDowell et al. 2016). Asymmetric repression of *dand5* mRNA by the flow signal leads to activation of the Nodal signaling pathway on the left but not the right side of KV. This asymmetric Nodal signal spreads to the left lateral plate mesoderm (LPM) and propagates anteriorly through the embryo (Long, Ahmad, and Rebagliati 2003; Shiratori and Hamada 2014).

Symmetry breaking is dependent on the Polycystin protein, Pkd1l1 in mouse, medaka fish, zebrafish, and humans (Field et al. 2011; Grimes et al. 2016; Vetrini et al. 2016) (**Figure 1C**). Additionally, Pkd2 is required for L-R patterning (Bisgrove et al. 2005; Pennekamp et al. 2002). Pkd2 is a transient receptor potential ion channel that may mediate L-R patterning by flow induced Ca^{2+} spikes in flow sensory cells (Yuan et al. 2015). Pkd2 acts downstream of flow in the kidney, and forms a functional complex with the Pkd1l1 homolog, Pkd1 (Kamura et al. 2011). Mutations in PKD2 and PKD1 cause autosomal dominant polycystic kidney disease (Harris and Torres 2009; Igarashi and Somlo 2007). While it is clear that these proteins are required for flow signaling in several contexts, it is not understood how they function.

While we know that flow is critical for proper L-R patterning, very little is known about how the flow signal is sensed and transduced to ultimately result in asymmetric *dand5* repression. The zebrafish L-R patterning system, tractable to imaging and genetic manipulation, with a controllable flow input and quantifiable *dand5* output, is ideal for discovering basic principles of flow signaling.

Results

Sensation and transduction of the fluid flow signal is critical for establishing L-R asymmetry. However, few flow sensory pathway regulators are known. I performed a reverse genetic screen and discovered novel regulators of L-R patterning.

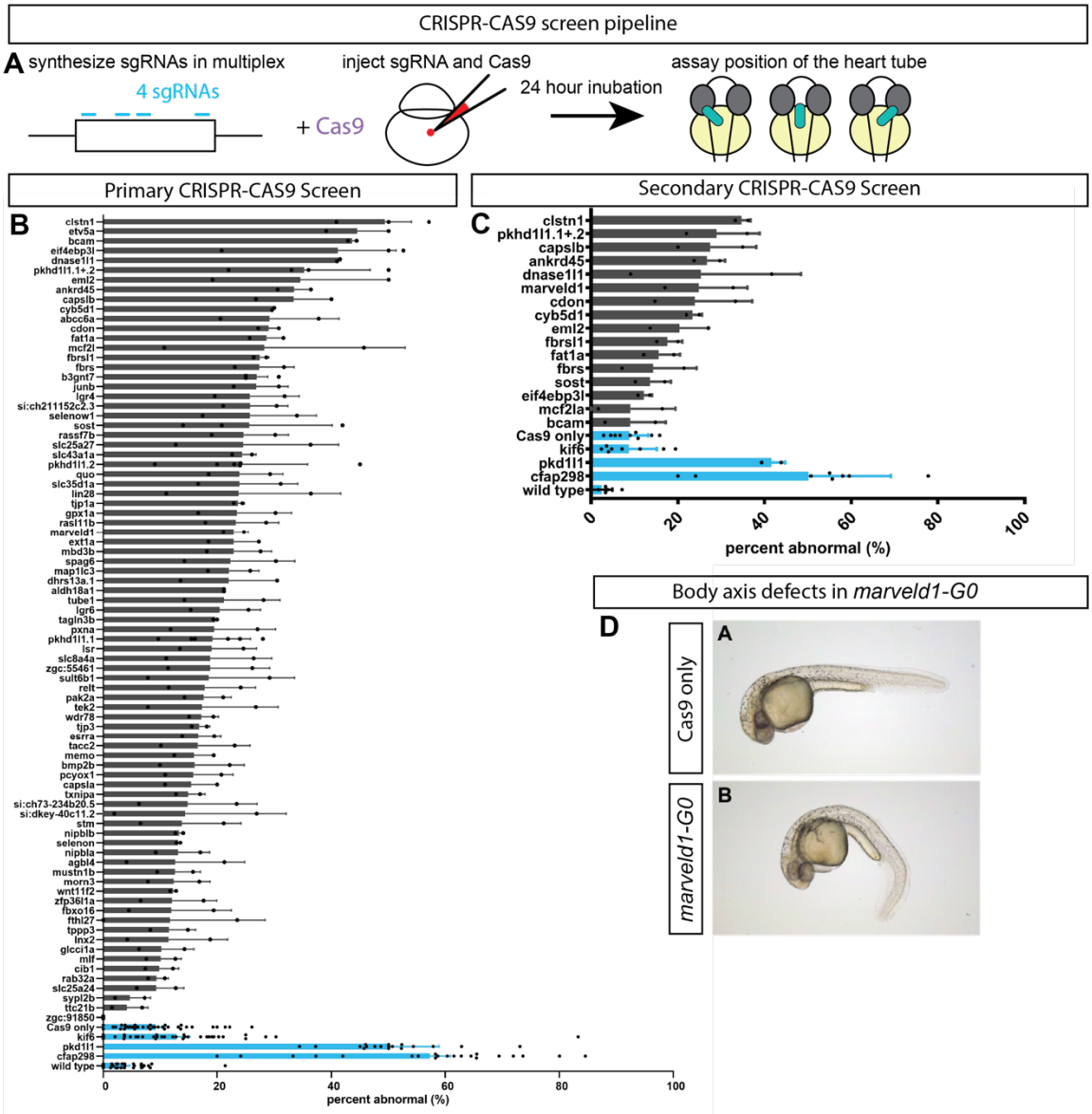

Figure 2. **Reverse genetics screen to identify regulators of L-R patterning.** A) schematic of CRISPR-CAS9 screen pipeline. Four single guides are generated in multiplex, then injected with Cas9 protein into one cell stage embryos, then embryos are raised for 24 hours at 28C. Heart tube positioning is then assessed. B) graph of percent abnormal heart jogging (middle or right) for each gene screened. C) a second set of guide RNAs was generated and injected for top hits to validate phenotypes. D) *marveld1* embryos displayed body shape defects indicated by the downward curve of the tail in addition to heart jogging defects.

Discovery of Novel Regulators of L-R Patterning. Using CRISPR-Cas9, I generated somatic mosaic (G0) mutants in zebrafish by targeting genes with a high concentration of four guide RNAs (gRNAs) (Wu et al. 2018) that target different regions of the same gene. With this technique, I generated loss-of-function-like phenotypes. To assess L-R patterning, I determined heart jogging, a reliable readout of L-R asymmetry, in embryos at 23 hours post fertilization (hpf) (**Figure 2A**). In wild-type embryos at 23 hpf, the heart is positioned to the left (Chen et al. 1997), and in embryos with disrupted L-R asymmetry, heart positioning is disrupted (i.e. randomized between left and right, or sometimes positioned in the middle) (Baker, Holtzman, and Burdine 2008; Smith et al. 2008).

I validated this method by targeting known regulators of L-R patterning. Targeting *dand5*, *pkd1l1*, and *cfap298*, which are expressed in KV and have previously been implicated in L-R patterning (Bisgrove et al. 2005; Jaffe et al. 2016) resulted in 30-90% levels of abnormal heart laterality (**Figure 2B**). *cfap298* also displayed a curved body axis, called curly-tail down, which phenocopied germline mutants (Jaffe et al. 2016). Additionally, we targeted a gene, *kif6,* that had no role in L-R patterning but has other visible body shape defects when knocked down (Buchan et al. 2014). These levels of heart defects, as well as those induced by Cas9 injection alone, served as a background for comparisons to novel genes. When assessing heart jogging, it is important to note that since the primary phenotype of L-R patterning mutants is randomization of laterality, 50% abnormalities could represent 100% penetrance of mutant phenotypes due to a randomization between left and right.

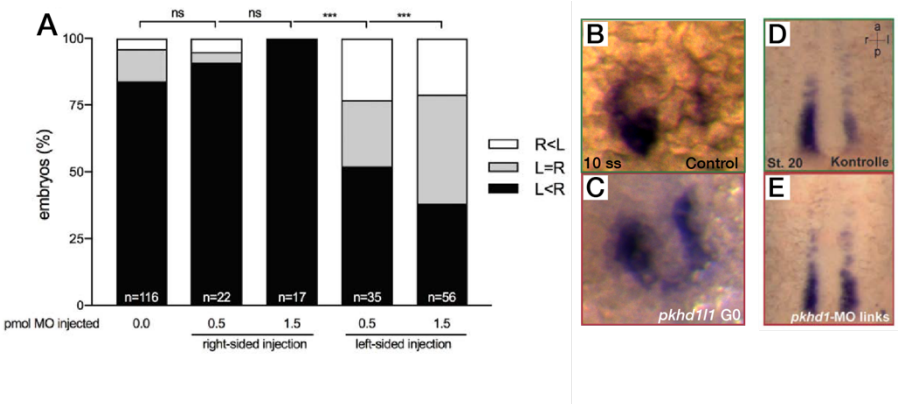

Fig 3. Fibrocystin is required for L-R patterning in zebrafish and *Xenopus*. B,D) double G0 *pkhd1l1.1* and *pkhd1l1.2* mutants display bilaterally symmetric L=R *dand5* in KV at 10 somite stage. **A,D,E)** *dand5* expression in the L-R organizer of stage 20 *Xenopus* is normally L<R, but morpholino knockdown of *pkhd1* in *Xenopus* on the left, but not right side results in abnormal *dand5* expression (E). ***p<0.5, ns p>0.05, Pearson chai-square test (Bonferonni corrected). [Kontrolle = Control, links = left]

195 genes as expressed in KV as of 2021 (ZFIN). Of these 195 genes, 78 have previously identified roles in L-R patterning and/or motile cilia function, and 27 have known roles in motile cilia in contexts outside of L-R patterning, leaving 90 genes with no known role in L-R patterning or cilia motility/formation. We generated multiplexed gRNAs against each gene, injected guide sets with two replicates per gene, and assayed heart jogging. We observed a broad range of L-R patterning defects ranging from 15-50% heart laterality defects seen. To validate the phenotypes we observed and control for potential off-target effects of specific gRNAs, we selected several genes that had reproducibly high percent phenotypes to generate a second set of multiplexed gRNAs (Figure 2C).

Fibrocystin regulates L-R patterning in somatic mutants in zebrafish and *Xenopus*

pkhd1l1 encodes Fibrocystin, which is implicated in polycystic kidney disease (Harris and Rossetti 2004; Harris and Torres 2009). In zebrafish, Fibrocystin is encoded by tandem repeats, *pkhd1l1.1* and *pkhd1l1.2*. I generated somatic mosaic mutants as described above and found L-R defects in mutants (**Fig 2C**). Targeting both repeats increased the levels of L-R defects. Additionally, we found that *dand5* asymmetry was disrupted in Fibrocystin somatic mutants (**Figure 3B-C**). Wild-type AB embryos show stronger expression of *dand5* on the right side. *pkhd1ll* double G0s embryos have right biased expression similar to WT but also have stronger expression on the left side as well, indicating decreased repression of *dand5* on the left side.

In *Xenopus*, we found *Pkhd1* (the ortholog of zebrafish *pkhd1l1*) is expressed in flow sensory cells in the L-R organizer (**Figure 4**). We targeted *Pkhd1* with morpholinos and found L-R defects (**Figure 3A**). We specifically targeted cells on the left or right side of the embryo and found that knockdown of *Pkhd1* on the right side had no effect on L-R patterning, whereas knockdown on the left side resulted in abnormal *dand5* asymmetry (**Figure 3D-E**). Since the left side is where flow represses *dand5*, this suggests that Fibrocystin functions to activate *dand5* repression.

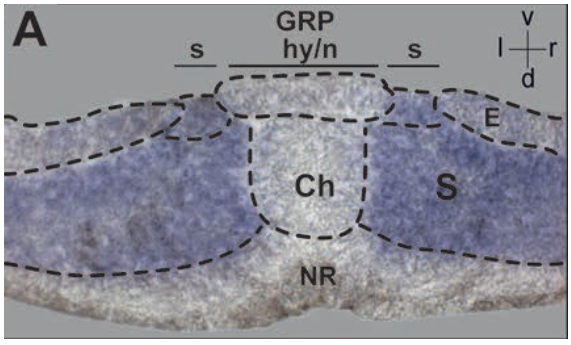

Figure 4. *pkhd1*expression in the *Xenopus* Left-Right organizer. s=sensory cells.

Germline mutants do not phenocopy somatic mosaic mutants

Upon a secondary screen through 16 genes, we selected four genes with reproducibly high phenotypes to generate whole-animal germline mutants for the following reasons:

clstn1 is predicted to have calcium-binding activity. Therefore, Clstn1 may moderate L-R patterning through the Ca^{2+} spikes in flow sensory cells induced by Pkd2 (McGrath et al. 2003; Yuan et al. 2015).

eml2 is predicted to enable microtubule-binding activity and is associated with signal receptor binding, and thus influence L-R patterning by altering the cytoskeleton or acting as a signaling protein (McDowell et al. 2016).

marveld1 is predicted to be involved in myelination. Intriguingly, *marveld1* G0 mutants displayed axial defects in addition to L-R defects (**Figure 2D**). This suggests *marveld1* may impact L-R patterning the cilia level, as cilia-driven flow is required for axial straightening in zebrafish (Baker, Holtzman, and Burdine 2008; Kramer-Zucker et al. 2005).

Pkhd1l1 or Fibrocystin, which is encoded by two tandem repeats in zebrafish, *pkhd1l1.1* and *pkhd1l1.2*, is associated with autosomal recessive polycystic kidney disease (ARPKD) (Harris and Torres 2009), a disease with significant clinical overlap with autosomal dominant polycystic kidney disease (ADPKD) cause by Polycystin mutations. Therefore, Fibrocystin may moderate L-R patterning through interactions with the Polycystin proteins Pkd1l1 and Pkd2.

Guides used to generate whole-animal germline mutants were selected from the 8 guides that had been used in the primary or secondary screen. To validate the CRISPR gRNAs selected to make germline mutants, I first injected two guides per gene at a high concentration along with Cas9 and observed heart laterality. If guides produced L-R defects, then the pairs of guides were injected at a lower concentration to induce mutations. Mutations were confirmed by PCR and restriction enzyme digestion.

We raised injected embryos and performed subsequent outcrosses to generate F3 homozygous adults. We bred pairs or groups of homozygous adults to generate homozygous mutant progeny and control for maternal effects. Surprisingly, we did not observe abnormal heart

jogging in *clstn1, eml2, marveld1,* or *pkhd1l1* mutant embryos (data not shown). In clutches of 30+ embryos, we scored low-to-near zero levels of heart jogging defects, matching wildtype levels of defects.

Discussion

Our findings pose conflicting phenotypic results between somatic mutants and whole animal mutants. In somatic mutants, L-R heart laterality defects happen at high frequency, but whole animal mutants had very low levels of L-R heart laterality defects. We hypothesize this may be due to a few factors. It is possible that L-R patterning defects in the heart are induced in somatic mutants due stress conditions. Mild cold stress has been shown to alter the movements of the dorsal forerunner cells (DFCs) that generate KV and altered DFC movement leads to disrupted KV formation and L-R patterning (Liu *et al*., 2022). Additionally, CRISPR-Cas9 induced mutations in embryos generates mosaic embryos as the mutations are not always triggered as early as the one cell stage. Therefore, phenotypes induced in G0 mutants could be due to mosaicism in KV. Disruptions in varying amounts of cells in KV at random positions around the sphere may be enough to disrupt flow or flow sensation and induce L-R defects.

Another possibility is differences in genetic compensation between somatic mutants and germline mutants. Reverse genetics screens with morpholinos (MO) in zebrafish, mice, and *Arabidopsis* have shown that there can also be differences between genetic mutants and gene knockdown, where genetic mutants display mild or no phenotypes, and morphants display more severe phenotypes (Daude et al. 2012; De Souza et al. 2006; Gao et al. 2015; Kok et al. 2015; Law and Sargent 2014; Smart and Riley 2013; Stainier, Kontarakis, and Rossi 2015). Previous work shown that deleterious mutations can induce upregulation of similar genes to compensate for the lack of the originally deleted gene, however, this is not detected in morphants with transcriptional or translational knockdown (Rossi et al. 2015). Further research has demonstrated that alleles that transcribe the mutated gene are able to induce genetic compensation, while true nulls that generate no transcript do not induce genetic compensation (El-Brolosy et al. 2019). Mutations were induced as early as possible within the first few exons of our germline mutants and thus transcriptional start sites likely are preserved. Therefore, genetic compensation could possibly explain the differences between G0 somatic mutants and germline mutants. It would be

interesting to understand if mutations induced through injection of multiplexed gRNAs is sufficient to trigger genetic compensation in zebrafish embryos.

Our results show that Fibrocystin may function in the L-R patterning pathway, with evidence in both zebrafish and *Xenopus*. Fibrocystin localizes to primary cilia, the basal body, and cytoplasm in cell lines (Menezes et al. 2004; Wang et al. 2004; Ward 2003). In mouse kidney, it physically interacts with Pkd2 and loss of either causes kidney cysts (Kim et al. 2008). In KV, Pkd2 interacts and colocalizes to cilia with Pkd1l1 (Kamura et al. 2011). Transcriptomic analysis between zebrafish germline mutants and control siblings will be informative to determine if genetic compensation is masking a mutant phenotype.

Methods

Generation of germline mutants

Embryos were injected with two single gRNA CRISPR guides at a concentration of 150µg/nl with Cas9 protein at the single cell stage. Embryos were raised and screened for mutations. I confirmed the guides induced mutations by PCR to amplifying around the cut site followed by restriction-enzyme digestion of the fragment. In embryos or fish where mutations were induced, the enzymes failed to digest the PCR fragment.

F0 adults were outcrossed to ABC WT and embryos were screened for mutations. Adult fish that produced progeny with mutations were selected as founders. F1 progeny were raised and then outcrossed to ABC WT to isolate specific alleles. F2 heterozygous progeny were generated and then incrossed to generate F3 homozogous adults. F3 adults were incrossed to generate maternal-zygotic mutant progeny for analysis.

Statistical considerations for the L-R screen

As heart positioning is nominal, square tests to determine significance. I performed power analyses to determine the number of embryos needed to assess significance. I assumed an instance of abnormality at 5% for controls and 66% for injected, based on the rates across validation experiments. From this, I calculated the sample size to be 26 individuals per group, with significance level alpha=0.05 and power=95%. In my screen, I performed two injection

replicates per gene, and injected at least 30 embryos per replicate, giving around 60 embryos per group, which is above the 26 required for statistical power.

CHAPTER IV

DISCUSSION

Overall, this work demonstrates a role for RNA-binding proteins and transcription factors in aspects of morphological identity of motor neurons in the *Drosophila* CNS. While we demonstrate roles for Imp and Chinmo in specifying morphological identity in motor neurons, we hypothesize that these genes may also have roles in morphological identity in interneurons. It would be interesting to understand if Imp and Chinmo play roles molecular identity in interneurons or if this is only observed in larval stages. Future work understanding the role of Imp, Chinmo, and Sequoia in interneurons will add to our knowledge or neuronal specification and identity more broadly.

We found that Imp and Chinmo knockdown caused opposing phenotypes in motor neuron axons and dendrites. While dendrites showed an increase in arborization with ectopic growth into the midline, axons showed decreased growth with axons not extending out to their target muscles. A similar phenotype has been seen in *sequoia* mutants in multidendritic sensory neurons. It would be interesting to understand how both over and under growth of axons and dendrites is achievable in the motor neurons. Further, understanding the behavior consequences of these morphological changes would be critical to understanding the functional role of these ectopic dendrites and improperly targeted axons. To understand the functional role of Imp and Chinmo, future work to know of these dendrites and axons for functional synapses will also be critical.

APPENDIX

Appendix A. Chapter I supplementary figures

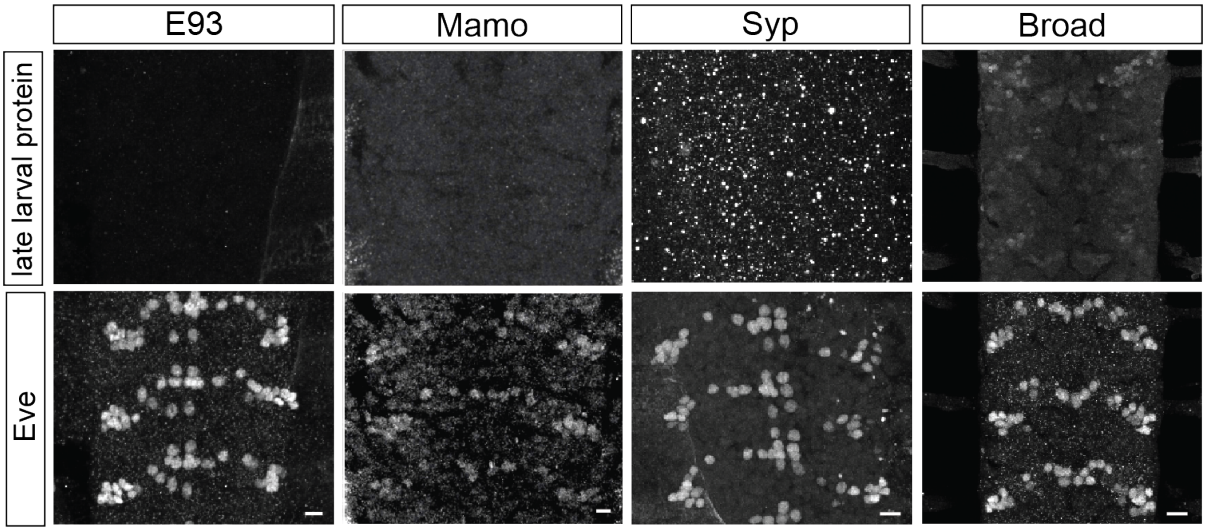

Supplemental figure 1. Late larval proteins show little or no expression in embryos. Syp, Mamo, E93, are not expressed in the embryonic VNC. Br is expressed in embryonic neurons, but in a subset of cells rather than a gradient. Eve is shown as a fiduciary marker for a subset of post-mitotic motoneurons and interneurons. Stage 17 shown; anterior up; scale bar 5μm.

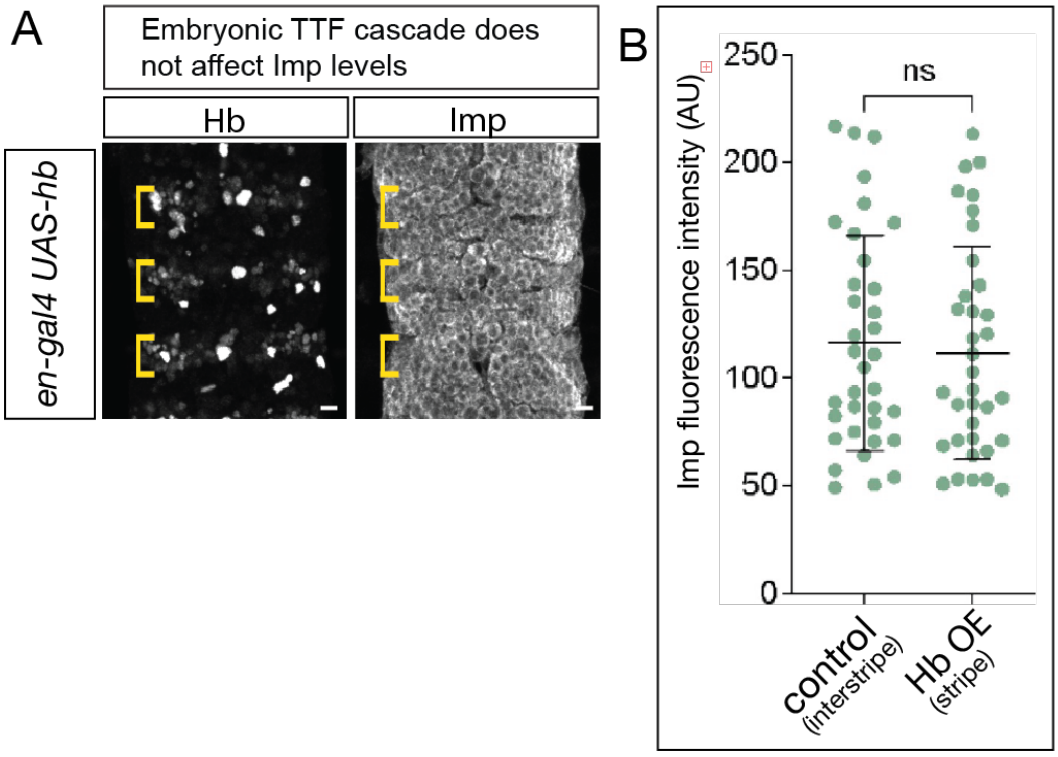

Supplemental figure 2. The embryonic TTF cascade does not affect Imp levels
(A-B) Overexpression of Hb does not alter Imp expression. (A) Hb is overexpressed in a stripe pattern via *en-gal4 UAS-hb*. Control, interstripe domain; Hb overexpression, stripe domain (brackets). (B) Quantification. n > 9 embryos. Ventral view. Scale bar = 5μM

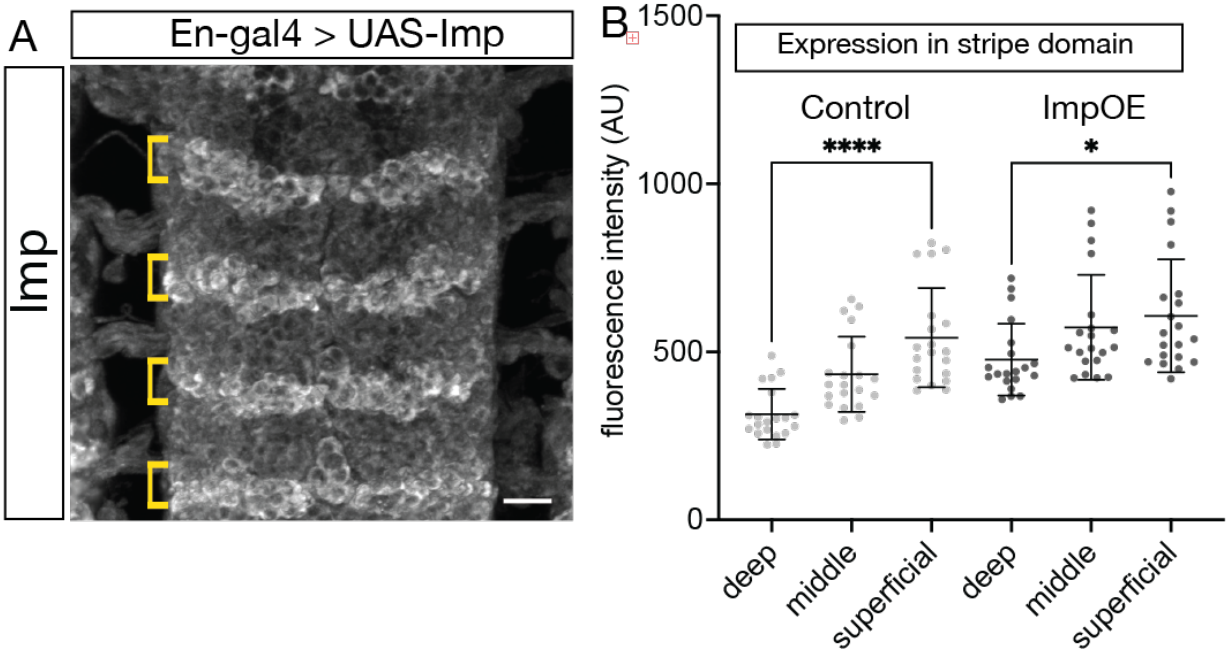

Supplemental Figure 3. Imp overexpression can flatten the Imp gradient.
(A) Imp overexpression in stripes (brackets) via *en-gal4 UAS-Imp* transgene. Ventral view, anterior up, scale bar, 10µm. (B) Imp overexpression leads to a flattening of the Imp gradient within the stripe domain.

REFERENCES

Adolph, Sidsel Kramshøj, Robert DeLotto, Finn Cilius Nielsen, and Jan Christiansen. 2009. "Embryonic Expression of Drosophila IMP in the Developing CNS and PNS." *Gene Expression Patterns: GEP* 9 (3): 138–43. https://doi.org/10.1016/j.gep.2008.12.001.

Baker, Kari, Nathalia G Holtzman, and Rebecca D Burdine. 2008. "Direct and Indirect Roles for Nodal Signaling in Two Axis Conversions during Asymmetric Morphogenesis of the Zebrafish Heart." *Proceedings of the National Academy of Sciences of the United States of America* 105 (37): 13924–29. https://doi.org/10.1073/pnas.0802159105.

Bayraktar, O. A., and C. Q. Doe. 2013. "Combinatorial Temporal Patterning in Progenitors Expands Neural Diversity." *Nature* 498 (June):445–55. https://doi.org/10.1038/nature12266.

Bello, B. C., N. Izergina, E. Caussinus, and H. Reichert. 2008. "Amplification of Neural Stem Cell Proliferation by Intermediate Progenitor Cells in Drosophila Brain Development." *Neural Dev* 3:5. https://doi.org/10.1186/1749-8104-3-5.

Bisgrove, Brent W., Brian S. Snarr, Anoush Emrazian, and H. Joseph Yost. 2005. "Polaris and Polycystin-2 in Dorsal Forerunner Cells and Kupffer's Vesicle Are Required for Specification of the Zebrafish Left–Right Axis." *Developmental Biology* 287 (2): 274–88. https://doi.org/10.1016/j.ydbio.2005.08.047.

Boone, J. Q., and C. Q. Doe. 2008. "Identification of Drosophila Type II Neuroblast Lineages Containing Transit Amplifying Ganglion Mother Cells." *Dev Neurobiol* 68 (9): 1185–95. https://doi.org/10.1002/dneu.20648.

Bowman, S. K., V. Rolland, J. Betschinger, K. A. Kinsey, G. Emery, and J. A. Knoblich. 2008. "The Tumor Suppressors Brat and Numb Regulate Transit-Amplifying Neuroblast Lineages in Drosophila." *Dev Cell* 14 (4): 535–46. https://doi.org/10.1016/j.devcel.2008.03.004.

Boylan, Kristin L. M., Sarah Mische, Mingang Li, Guillermo Marqués, Xavier Morin, William Chia, and Thomas S. Hays. 2008. "Motility Screen Identifies Drosophila IGF-II mRNA-Binding Protein—Zipcode-Binding Protein Acting in Oogenesis and Synaptogenesis." *PLOS Genetics* 4 (2): e36. https://doi.org/10.1371/journal.pgen.0040036.

Brenman, Jay E., Fen-Biao Gao, Lily Yeh Jan, and Yuh Nung Jan. 2001. "Sequoia, a Tramtrack-Related Zinc Finger Protein, Functions as a Pan-Neural Regulator for Dendrite and Axon

Morphogenesis in *Drosophila*." *Developmental Cell* 1 (5): 667–77. https://doi.org/10.1016/S1534-5807(01)00072-7.

Buchan, Jillian G, Ryan S Gray, John M Gansner, David M Alvarado, Lydia Burgert, Jonathan D Gitlin, Christina A Gurnett, and Matthew I Goldsmith. 2014. "Kinesin Family Member 6 (Kif6) Is Necessary for Spine Development in Zebrafish." *Developmental Dynamics : An Official Publication of the American Association of Anatomists* 243 (12): 1646–57. https://doi.org/10.1002/dvdy.24208.

Chen, Jau-Nian, Fredericus J. M. van Eeden, Kerri S. Warren, Alvin Chin, Christiane Nüsslein-Volhard, Pascal Haffter, and Mark C. Fishman. 1997. "Left-Right Pattern of Cardiac BMP4 May Drive Asymmetry of the Heart in Zebrafish." *Development* 124 (21): 4373–82. https://doi.org/10.1242/dev.124.21.4373.

Crews, Stephen T. 2019. "Drosophila Embryonic CNS Development: Neurogenesis, Gliogenesis, Cell Fate, and Differentiation." *Genetics* 213 (4): 1111–44. https://doi.org/10.1534/genetics.119.300974.

Daude, Nathalie, Serene Wohlgemuth, Rebecca Brown, Rose Pitstick, Hristina Gapeshina, Jing Yang, George A. Carlson, and David Westaway. 2012. "Knockout of the Prion Protein (PrP)-like Sprn Gene Does Not Produce Embryonic Lethality in Combination with PrP(C)-Deficiency." *Proceedings of the National Academy of Sciences of the United States of America* 109 (23): 9035–40. https://doi.org/10.1073/pnas.1202130109.

De Souza, Angus T., Xudong Dai, Andrew G. Spencer, Tom Reppen, Ann Menzie, Paula L. Roesch, Yudong He, et al. 2006. "Transcriptional and Phenotypic Comparisons of Ppara Knockout and siRNA Knockdown Mice." *Nucleic Acids Research* 34 (16): 4486–94. https://doi.org/10.1093/nar/gkl609.

Dillon, Noah R., and Chris Q. Doe. 2024. "Castor Is a Temporal Transcription Factor That Specifies Early Born Central Complex Neuron Identity." *Development (Cambridge, England)*, December, dev.204318. https://doi.org/10.1242/dev.204318.

Doe, C. Q. 2017. "Temporal Patterning in the Drosophila CNS." *Annu. Rev. Cell Dev. Biol.* 33:219–40. https://doi.org/PMID: 28992439.

El-Brolosy, Mohamed A., Zacharias Kontarakis, Andrea Rossi, Carsten Kuenne, Stefan Günther, Nana Fukuda, Khrievono Kikhi, et al. 2019. "Genetic Compensation Triggered by

Mutant mRNA Degradation." *Nature* 568 (7751): 193–97. https://doi.org/10.1038/s41586-019-1064-z.

El-Danaf, Rana N., Raghuvanshi Rajesh, and Claude Desplan. 2023. "Temporal Regulation of Neural Diversity in Drosophila and Vertebrates." *Seminars in Cell & Developmental Biology* 142 (June):13–22. https://doi.org/10.1016/j.semcdb.2022.05.011.

Erclik, T., X. Li, M. Courgeon, C. Bertet, Z. Chen, R. Baumert, J. Ng, et al. 2017. "Integration of Temporal and Spatial Patterning Generates Neural Diversity." *Nature* 541 (7637): 365–70. https://doi.org/10.1038/nature20794.

Essner, Jeffrey J., Jeffrey D. Amack, Molly K. Nyholm, Erin B. Harris, and H. Joseph Yost. 2005. "Kupffer's Vesicle Is a Ciliated Organ of Asymmetry in the Zebrafish Embryo That Initiates Left-Right Development of the Brain, Heart and Gut." *Development* 132 (6): 1247–60. https://doi.org/10.1242/dev.01663.

Feng, Yanfei, Atsushi Ueda, and Chun-Fang Wu. 2004. "A Modified Minimal Hemolymph-like Solution, HL3.1, for Physiological Recordings at the Neuromuscular Junctions of Normal and Mutant Drosophila Larvae." *Journal of Neurogenetics* 18 (2): 377–402. https://doi.org/10.1080/01677060490894522.

Field, Sarah, Kerry-Lyn Riley, Daniel T Grimes, Helen Hilton, Michelle Simon, Nicola Powles-Glover, Pam Siggers, Debora Bogani, Andy Greenfield, and Dominic P Norris. 2011. "Pkd1l1 Establishes Left-Right Asymmetry and Physically Interacts with Pkd2." *Development (Cambridge, England)* 138 (6): 1131–42. https://doi.org/10.1242/dev.058149.

Freund, Jonathan B, Jacky G Goetz, Kent L Hill, and Julien Vermot. 2012. "Fluid Flows and Forces in Development: Functions, Features and Biophysical Principles." *Development (Cambridge, England)* 139 (7): 1229–45. https://doi.org/10.1242/dev.073593.

Gao, Yangbin, Yi Zhang, Da Zhang, Xinhua Dai, Mark Estelle, and Yunde Zhao. 2015. "Auxin Binding Protein 1 (ABP1) Is Not Required for Either Auxin Signaling or Arabidopsis Development." *Proceedings of the National Academy of Sciences of the United States of America* 112 (7): 2275–80. https://doi.org/10.1073/pnas.1500365112.

Grimes, Daniel T, and Rebecca D Burdine. 2017. "Left-Right Patterning: Breaking Symmetry to Asymmetric Morphogenesis." *Trends in Genetics : TIG* 33 (9): 616–28. https://doi.org/10.1016/j.tig.2017.06.004.

Grimes, Daniel T, Jennifer L Keynton, Maria T Buenavista, Xingjian Jin, Saloni H Patel, Shinohara Kyosuke, Jennifer Vibert, et al. 2016. “Genetic Analysis Reveals a Hierarchy of Interactions between Polycystin-Encoding Genes and Genes Controlling Cilia Function during Left-Right Determination.” *PLoS Genetics* 12 (6): e1006070–e1006070. https://doi.org/10.1371/journal.pgen.1006070.

Grueber, Wesley B., Lily Y. Jan, and Yuh Nung Jan. 2002. “Tiling of the Drosophila Epidermis by Multidendritic Sensory Neurons.” *Development* 129 (12): 2867–78. https://doi.org/10.1242/dev.129.12.2867.

Guan, Wenyue, Stéphanie Bellemin, Mathilde Bouchet, Lalanti Venkatasubramanian, Camille Guillermin, Anne Laurençon, Chérif Kabir, et al. 2022. “Post-Transcriptional Regulation of Transcription Factor Codes in Immature Neurons Drives Neuronal Diversity.” *Cell Reports* 39 (13): 110992. https://doi.org/10.1016/j.celrep.2022.110992.

Guillemot, F. 2007. “Spatial and Temporal Specification of Neural Fates by Transcription Factor Codes.” *Development* 134 (21): 3771–80. https://doi.org/dev.006379 [pii] 10.1242/dev.006379.

Hamid, Aisha, Hannah Gattuso, Aysu Nora Caglar, Midhula Pillai, Theresa Steele, Alexa Gonzalez, Katherine Nagel, and Mubarak Hussain Syed. 2024. “The Conserved RNA-Binding Protein Imp Is Required for the Specification and Function of Olfactory Navigation Circuitry in Drosophila.” *Current Biology: CB* 34 (3): 473-488.e6. https://doi.org/10.1016/j.cub.2023.12.020.

Harris, Peter C, and Sandro Rossetti. 2004. “Molecular Genetics of Autosomal Recessive Polycystic Kidney Disease.” *Molecular Genetics and Metabolism* 81 (2): 75–85. https://doi.org/10.1016/j.ymgme.2003.10.010.

Harris, Peter C, and Vicente E Torres. 2009. “Polycystic Kidney Disease.” *Annual Review of Medicine* 60:321–37. https://doi.org/10.1146/annurev.med.60.101707.125712.

Hoffman, Julien I.E, and Samuel Kaplan. 2002. “The Incidence of Congenital Heart Disease.” *Journal of the American College of Cardiology* 39 (12): 1890–1900. https://doi.org/10.1016/s0735-1097(02)01886-7.

Hojo, Motoki, Shigeo Takashima, Daisuke Kobayashi, Akira Sumeragi, Atsuko Shimada, Tatsuya Tsukahara, Hayato Yokoi, et al. 2007. “Right-elevated Expression of Charon Is

Regulated by Fluid Flow in Medaka Kupffer's Vesicle." *Development, Growth & Differentiation* 49 (5): 395–405. https://doi.org/10.1111/j.1440-169x.2007.00937.x.

Homem, C. C., I. Reichardt, C. Berger, T. Lendl, and J. A. Knoblich. 2013. "Long-Term Live Cell Imaging and Automated 4D Analysis of Drosophila Neuroblast Lineages." *PLoS One* 8 (11): e79588. https://doi.org/10.1371/journal.pone.0079588.

Igarashi, Peter, and Stefan Somlo. 2007. "Polycystic Kidney Disease." *Journal of the American Society of Nephrology* 18 (5): 1371–73. https://doi.org/10.1681/asn.2007030299.

Islam, Ishrat Maliha, and Ted Erclik. 2022. "Imp and Syp Mediated Temporal Patterning of Neural Stem Cells in the Developing Drosophila CNS." *Genetics* 222 (1): iyac103. https://doi.org/10.1093/genetics/iyac103.

Isshiki, T., B. Pearson, S. Holbrook, and C. Q. Doe. 2001. "Drosophila Neuroblasts Sequentially Express Transcription Factors Which Specify the Temporal Identity of Their Neuronal Progeny." *Cell* 106 (4): 511–21. https://doi.org/PMID: 11525736.

Isshiki, Takako, Bret Pearson, Scott Holbrook, and Chris Q. Doe. 2001. "*Drosophila* Neuroblasts Sequentially Express Transcription Factors Which Specify the Temporal Identity of Their Neuronal Progeny." *Cell* 106 (4): 511–21. https://doi.org/10.1016/S0092-8674(01)00465-2.

Jaffe, Kimberly M, Daniel T Grimes, Jodi Schottenfeld-Roames, Michael E Werner, Tse-Shuen J Ku, Sun K Kim, Jose L Pelliccia, Nicholas F C Morante, Brian J Mitchell, and Rebecca D Burdine. 2016. "C21orf59/Kurly Controls Both Cilia Motility and Polarization." *Cell Reports* 14 (8): 1841–49. https://doi.org/10.1016/j.celrep.2016.01.069.

Kamura, Keiichiro, Daisuke Kobayashi, Yuka Uehara, Sumito Koshida, Norio Iijima, Akira Kudo, Takahiko Yokoyama, and Hiroyuki Takeda. 2011. "Pkd1l1 Complexes with Pkd2 on Motile Cilia and Functions to Establish the Left-Right Axis." *Development* 138 (6): 1121–29. https://doi.org/10.1242/dev.058271.

Kim, Ingyu, Yulong Fu, Kwokyin Hui, Gilbert Moeckel, Weiyi Mai, Cunxi Li, Dan Liang, et al. 2008. "Fibrocystin/Polyductin Modulates Renal Tubular Formation by Regulating Polycystin-2 Expression and Function." *Journal of the American Society of Nephrology : JASN* 19 (3): 455–68. https://doi.org/10.1681/ASN.2007070770.

Kok, F. O., M. Shin, C.-W. Ni, A. Gupta, A. S. Grosse, A. van Impel, B. C. Kirchmaier, et al. 2015. "Reverse Genetic Screening Reveals Poor Correlation between Morpholino-

Induced and Mutant Phenotypes in Zebrafish." *Developmental Cell* 32 (1): 97–108. https://doi.org/10.1016/j.devcel.2014.11.018.

Kothari, Shyam S. 2014. "Non-Cardiac Issues in Patients with Heterotaxy Syndrome." *Annals of Pediatric Cardiology* 7 (3): 187–92. https://doi.org/10.4103/0974-2069.140834.

Kramer-Zucker, Albrecht G., Felix Olale, Courtney J. Haycraft, Bradley K. Yoder, Alexander F. Schier, and Iain A. Drummond. 2005. "Cilia-Driven Fluid Flow in the Zebrafish Pronephros, Brain and Kupffer's Vesicle Is Required for Normal Organogenesis." *Development* 132 (8): 1907–21. https://doi.org/10.1242/dev.01772.

Law, Sheran H. W., and Thomas D. Sargent. 2014. "The Serine-Threonine Protein Kinase PAK4 Is Dispensable in Zebrafish: Identification of a Morpholino-Generated Pseudophenotype." *PLOS ONE* 9 (6): e100268. https://doi.org/10.1371/journal.pone.0100268.

Liu, Ling-Yu, Xi Long, Ching-Po Yang, Rosa L. Miyares, Ken Sugino, Robert H. Singer, and Tzumin Lee. 2019. "Mamo Decodes Hierarchical Temporal Gradients into Terminal Neuronal Fate." *eLife* 8 (September):e48056. https://doi.org/10.7554/eLife.48056.

Liu, Z., C. P. Yang, K. Sugino, C. C. Fu, L. Y. Liu, X. Yao, L. P. Lee, and T. Lee. 2015. "Opposing Intrinsic Temporal Gradients Guide Neural Stem Cell Production of Varied Neuronal Fates." *Science* 350 (6258): 317–20. https://doi.org/10.1126/science.aad1886.

Long, Sarah, Nadira Ahmad, and Michael Rebagliati. 2003. "The Zebrafishnodal-Related Genesouthpawis Required for Visceral and Diencephalic Left-Right Asymmetry." *Development* 130 (11): 2303–16. https://doi.org/10.1242/dev.00436.

Mark, Brandon, Sen-Lin Lai, Aref Arzan Zarin, Laurina Manning, Heather Q. Pollington, Ashok Litwin-Kumar, Albert Cardona, James W. Truman, and Chris Q. Doe. 2021. "A Developmental Framework Linking Neurogenesis and Circuit Formation in the Drosophila CNS." *eLife* 10 (May):e67510. https://doi.org/10.7554/eLife.67510.

Matsui, Takaaki, and Yasumasa Bessho. 2012. "Left-Right Asymmetry in Zebrafish." *Cellular and Molecular Life Sciences : CMLS* 69 (18): 3069–77. https://doi.org/10.1007/s00018-012-0985-6.

Mattar, Pierre, and Michel Cayouette. 2015. "Mechanisms of Temporal Identity Regulation in Mouse Retinal Progenitor Cells." *Neurogenesis (Austin, Tex.)* 2 (1): e1125409. https://doi.org/10.1080/23262133.2015.1125409.

McDowell, Gary S, Joan M Lemire, Jean-Francois Paré, Garrett Cammarata, Laura Anne Lowery, and Michael Levin. 2016. “Conserved Roles for Cytoskeletal Components in Determining Laterality.” *Integrative Biology : Quantitative Biosciences from Nano to Macro* 8 (3): 267–86. https://doi.org/10.1039/c5ib00281h.

McGrath, James, Stefan Somlo, Svetlana Makova, Xin Tian, and Martina Brueckner. 2003. “Two Populations of Node Monocilia Initiate Left-Right Asymmetry in the Mouse.” *Cell* 114 (1): 61–73. https://doi.org/10.1016/s0092-8674(03)00511-7.

Menezes, Luís F.C., Yiqiang Cai, Yasuyuki Nagasawa, Ana M.G. Silva, Mary L. Watkins, Aline M. Da Silva, Stefan Somlo, Lisa M. Guay-Woodford, Gregory G. Germino, and Luiz F. Onuchic. 2004. “Polyductin, the PKHD1 Gene Product, Comprises Isoforms Expressed in Plasma Membrane, Primary Cilium, and Cytoplasm.” *Kidney International* 66 (4): 1345–55. https://doi.org/10.1111/j.1523-1755.2004.00844.x.

Nonaka, Shigenori, Hidetaka Shiratori, Yukio Saijoh, and Hiroshi Hamada. 2002. “Determination of Left–Right Patterning of the Mouse Embryo by Artificial Nodal Flow.” *Nature* 418 (6893): 96–99. https://doi.org/10.1038/nature00849.

Pennekamp, Petra, Christina Karcher, Anja Fischer, Axel Schweickert, Boris Skryabin, Jürgen Horst, Martin Blum, and Bernd Dworniczak. 2002. “The Ion Channel Polycystin-2 Is Required for Left-Right Axis Determination in Mice.” *Current Biology* 12 (11): 938–43. https://doi.org/10.1016/s0960-9822(02)00869-2.

Petrovic, Milan, and Thomas Hummel. 2008. “Temporal Identity in Axonal Target Layer Recognition.” *Nature* 456 (7223): 800–803. https://doi.org/10.1038/nature07407.

Pollington, Heather Q., and Chris Q. Doe. 2025. “The Hunchback Transcription Factor Determines Interneuron Molecular Identity, Morphology, and Presynapse Targeting in the Drosophila NB5-2 Lineage.” *PLoS Biology* 23 (3): e3002881. https://doi.org/10.1371/journal.pbio.3002881.

Pollington, Heather Q., Austin Q. Seroka, and Chris Q. Doe. 2023. “From Temporal Patterning to Neuronal Connectivity in Drosophila Type I Neuroblast Lineages.” *Seminars in Cell & Developmental Biology* 142 (June):4–12. https://doi.org/10.1016/j.semcdb.2022.05.022.

Ren, Qingzhong, Ching-Po Yang, Zhiyong Liu, Ken Sugino, Kent Mok, Yisheng He, Masayoshi Ito, Aljoscha Nern, Hideo Otsuna, and Tzumin Lee. 2017. “Stem Cell-Intrinsic, Seven-

up-Triggered Temporal Factor Gradients Diversify Intermediate Neural Progenitors." *Current Biology: CB* 27 (9): 1303–13. https://doi.org/10.1016/j.cub.2017.03.047.

Rossi, Andrea, Zacharias Kontarakis, Claudia Gerri, Hendrik Nolte, Soraya Hölper, Marcus Krüger, and Didier Y. R. Stainier. 2015. "Genetic Compensation Induced by Deleterious Mutations but Not Gene Knockdowns." *Nature* 524 (7564): 230–33. https://doi.org/10.1038/nature14580.

Sagner, A., and J. Briscoe. 2019. "Establishing Neuronal Diversity in the Spinal Cord: A Time and a Place." *Development* 146 (22). https://doi.org/10.1242/dev.182154.

Sagner, Andreas, Isabel Zhang, Thomas Watson, Jorge Lazaro, Manuela Melchionda, and James Briscoe. 2021. "A Shared Transcriptional Code Orchestrates Temporal Patterning of the Central Nervous System." *PLoS Biology* 19 (11): e3001450. https://doi.org/10.1371/journal.pbio.3001450.

Samuels, Tamsin J., Aino I. Järvelin, David Ish-Horowicz, and Ilan Davis. 2020. "Imp/IGF2BP Levels Modulate Individual Neural Stem Cell Growth and Division through Myc mRNA Stability." *eLife* 9 (January):e51529. https://doi.org/10.7554/eLife.51529.

Schweickert, Axel, Philipp Vick, Maike Getwan, Thomas Weber, Isabelle Schneider, Melanie Eberhardt, Tina Beyer, Anke Pachur, and Martin Blum. 2010. "The Nodal Inhibitor *Coco* Is a Critical Target of Leftward Flow in *Xenopus*." *Current Biology* 20 (8): 738–43. https://doi.org/10.1016/j.cub.2010.02.061.

Seroka, Austin, Rita M. Yazejian, Sen-Lin Lai, and Chris Q. Doe. 2020. "A Novel Temporal Identity Window Generates Alternating Eve+/Nkx6+ Motor Neuron Subtypes in a Single Progenitor Lineage." *Neural Development* 15 (1): 9. https://doi.org/10.1186/s13064-020-00146-6.

Shinohara, Kyosuke, and Hiroshi Hamada. 2017. "Cilia in Left-Right Symmetry Breaking." *Cold Spring Harbor Perspectives in Biology* 9 (10): a028282. https://doi.org/10.1101/cshperspect.a028282.

Shiratori, Hidetaka, and Hiroshi Hamada. 2014. "TGFβ Signaling in Establishing Left–Right Asymmetry." *Seminars in Cell & Developmental Biology* 32 (August):80–84. https://doi.org/10.1016/j.semcdb.2014.03.029.

Smart, Nicola, and Paul R. Riley. 2013. “Thymosin B4 in Vascular Development Response to Research Commentary.” *Circulation Research* 112 (3): e29-30. https://doi.org/10.1161/CIRCRESAHA.112.300555.

Smith, Kelly A., Sonja Chocron, Sophia von der Hardt, Emma de Pater, Alexander Soufan, Jeroen Bussmann, Stefan Schulte-Merker, Matthias Hammerschmidt, and Jeroen Bakkers. 2008. “Rotation and Asymmetric Development of the Zebrafish Heart Requires Directed Migration of Cardiac Progenitor Cells.” *Developmental Cell* 14 (2): 287–97. https://doi.org/10.1016/j.devcel.2007.11.015.

Stainier, Didier Y. R., Zacharias Kontarakis, and Andrea Rossi. 2015. “Making Sense of Anti-Sense Data.” *Developmental Cell* 32 (1): 7–8. https://doi.org/10.1016/j.devcel.2014.12.012.

Sullivan, Luis F, Timothy L Warren, and Chris Q Doe. 2019. “Temporal Identity Establishes Columnar Neuron Morphology, Connectivity, and Function in a Drosophila Navigation Circuit.” Edited by K VijayRaghavan. *eLife* 8 (February):e43482. https://doi.org/10.7554/eLife.43482.

Sutherland, Mardi J., and Stephanie M. Ware. 2009. “Disorders of Left–Right Asymmetry: Heterotaxy and Situs Inversus.” *American Journal of Medical Genetics Part C: Seminars in Medical Genetics* 151C (4): 307–17. https://doi.org/10.1002/ajmg.c.30228.

Syed, M. H., B. Mark, and C. Q. Doe. 2017. “Steroid Hormone Induction of Temporal Gene Expression in Drosophila Brain Neuroblasts Generates Neuronal and Glial Diversity.” *Elife* 6 (April). https://doi.org/10.7554/eLife.26287.

Tang, Jocelyn L. Y., Anna E. Hakes, Robert Krautz, Takumi Suzuki, Esteban G. Contreras, Paul M. Fox, and Andrea H. Brand. 2022. “NanoDam Identifies Homeobrain (ARX) and Scarecrow (NKX2.1) as Conserved Temporal Factors in the Drosophila Central Brain and Visual System.” *Developmental Cell* 57 (9): 1193-1207.e7. https://doi.org/10.1016/j.devcel.2022.04.008.

Titlow, Joshua, Francesca Robertson, Aino Järvelin, David Ish-Horowicz, Carlas Smith, Enrico Gratton, and Ilan Davis. 2020. “Syncrip/hnRNP Q Is Required for Activity-Induced Msp300/Nesprin-1 Expression and New Synapse Formation.” *The Journal of Cell Biology* 219 (3): e201903135. https://doi.org/10.1083/jcb.201903135.

Tran, K. D., and C. Q. Doe. 2008. “Pdm and Castor Close Successive Temporal Identity Windows in the NB3-1 Lineage.” *Development* 135 (21): 3491–99. https://doi.org/10.1242/dev.024349.

Tsuji, T., E. Hasegawa, and T. Isshiki. 2008. “Neuroblast Entry into Quiescence Is Regulated Intrinsically by the Combined Action of Spatial Hox Proteins and Temporal Identity Factors.” *Development* 135 (23): 3859–69. https://doi.org/10.1242/dev.025189.

Vetrini, Francesco, Lisa C A D’Alessandro, Zeynep C Akdemir, Alicia Braxton, Mahshid S Azamian, Mohammad K Eldomery, Kathryn Miller, et al. 2016. “Bi-Allelic Mutations in PKD1L1 Are Associated with Laterality Defects in Humans.” *American Journal of Human Genetics* 99 (4): 886–93. https://doi.org/10.1016/j.ajhg.2016.07.011.

Wang, Shixuan, Ying Luo, Patricia D. Wilson, George B. Witman, and Jing Zhou. 2004. “The Autosomal Recessive Polycystic Kidney Disease Protein Is Localized to Primary Cilia, with Concentration in the Basal Body Area.” *Journal of the American Society of Nephrology* 15 (3): 592–602. https://doi.org/10.1097/01.asn.0000113793.12558.1d.

Ward, C. J. 2003. “Cellular and Subcellular Localization of the ARPKD Protein; Fibrocystin Is Expressed on Primary Cilia.” *Human Molecular Genetics* 12 (20): 2703–10. https://doi.org/10.1093/hmg/ddg274.

Wreden, C. C., J. L. Meng, W. Feng, W. Chi, Z. D. Marshall, and E. S. Heckscher. 2017. “Temporal Cohorts of Lineage-Related Neurons Perform Analogous Functions in Distinct Sensorimotor Circuits.” *Curr Biol* 27 (10): 1521-1528.e4. https://doi.org/10.1016/j.cub.2017.04.024.

Wu, Roland S., Ian I. Lam, Hilary Clay, Daniel N. Duong, Rahul C. Deo, and Shaun R. Coughlin. 2018. “A Rapid Method for Directed Gene Knockout for Screening in G0 Zebrafish.” *Developmental Cell* 46 (1): 112-125.e4. https://doi.org/10.1016/j.devcel.2018.06.003.

Yang, Ching-Po, Tamsin J. Samuels, Yaling Huang, Lu Yang, David Ish-Horowicz, Ilan Davis, and Tzumin Lee. 2017. “Imp and Syp RNA-Binding Proteins Govern Decommissioning of Drosophila Neural Stem Cells.” *Development (Cambridge, England)* 144 (19): 3454–64. https://doi.org/10.1242/dev.149500.

Yoshiba, Satoko, Hidetaka Shiratori, Ivana Y Kuo, Aiko Kawasumi, Kyosuke Shinohara, Shigenori Nonaka, Yasuko Asai, et al. 2012. “Cilia at the Node of Mouse Embryos Sense

Fluid Flow for Left-Right Determination via Pkd2." *Science (New York, N.Y.)* 338 (6104): 226–31. https://doi.org/10.1126/science.1222538.

Yuan, Shiaulou, Lu Zhao, Martina Brueckner, and Zhaoxia Sun. 2015. "Intraciliary Calcium Oscillations Initiate Vertebrate Left-Right Asymmetry." *Current Biology : CB* 25 (5): 556–67. https://doi.org/10.1016/j.cub.2014.12.051.

Zhu, S., S. Lin, C. F. Kao, T. Awasaki, A. S. Chiang, and T. Lee. 2006. "Gradients of the Drosophila Chinmo BTB-Zinc Finger Protein Govern Neuronal Temporal Identity." *Cell* 127 (2): 409–22. https://doi.org/10.1016/j.cell.2006.08.045.